

Robust Decentralized Learning with Local Updates and Gradient Tracking

Sajjad Ghasvand	Amirhossein Reiszadeh	Mahnoosh Alizadeh	Ramtin Pedarsani
ECE Department	LIDS	ECE Department	ECE Department
UC Santa Barbara	MIT	UC Santa Barbara	UC Santa Barbara
sajjad@ucsb.edu	amirr@mit.edu	alizadeh@ece.ucsb.edu	ramtin@ece.ucsb.edu

Abstract

As distributed learning applications such as Federated Learning, the Internet of Things (IoT), and Edge Computing grow, it is critical to address the shortcomings of such technologies from a theoretical perspective. As an abstraction, we consider decentralized learning over a network of communicating clients or nodes and tackle two major challenges: *data heterogeneity* and *adversarial robustness*. We propose a decentralized minimax optimization method that employs two important modules: local updates and gradient tracking. Minimax optimization is the key tool to enable adversarial training for ensuring robustness. Having local updates is essential in Federated Learning (FL) applications to mitigate the communication bottleneck, and utilizing gradient tracking is essential to proving convergence in the case of data heterogeneity. We analyze the performance of the proposed algorithm, Dec-FedTrack, in the case of nonconvex-strongly-concave minimax optimization, and prove that it converges a stationary point. We also conduct numerical experiments to support our theoretical findings.

I. INTRODUCTION

Learning from distributed data is at the core of modern and successful technologies such as Internet of Things (IoT), Edge Computing, fleet learning, etc., where massive amounts of data are generated across dispersed users. Depending on the application, there are two main architectures for the learning paradigm: (i) A *distributed* setting with a central parameter server or master nodes that are responsible for aggregating the model and is able to communicate to all the computing nodes or workers; (ii) A *decentralized* setting for which there is no central coordinating node, and all the nodes communicate to their neighbors through a connected communicating graph. In this work, we focus on the latter.

Federated learning (FL) is a novel and promising distributed learning paradigm mostly employed using the master-worker architecture that aims to find accurate models across distributed nodes [1, 2]. The main premise of FL framework is user data privacy, that is, locally stored data on each entity remains local during the training procedure, which is in contrast to traditional distributed learning paradigms. In the peer-to-peer or decentralized implementation of FL methods which is the focus of this work, distributed nodes update model parameters locally using local optimization modules such as Stochastic Gradient Descent (SGD) and exchange information with their neighboring nodes to reach consensus. In Federated Learning, due to privacy and communication constraints, each communication round consists of *multiple local updates* before each node aggregates the neighboring updates.

While FL enables us to efficiently train a model, an important challenge is to ensure the robustness of the learned model to possible noisy/adversarial perturbations. The problem becomes more critical in FL since due to its distributed nature, it is more vulnerable to the presence of adversarial nodes and adversarial attacks. Adversarial training based on minimax optimization is the key tool to robustify the learned model in machine learning. Thus, it is critical to develop decentralized minimax optimization algorithms that are also communication-efficient, i.e. optimization methods that employ local updates suitable for a federated setting. Other applications of federated minimax optimization include using optimal transport to develop personalized FL [3] and robustness against distributed shifts [4]. Another major challenge in decentralized learning methods is data heterogeneity. Data heterogeneity refers to the fact that the data distributions across distributed nodes are statistically heterogeneous (or non-iid). In this work, we employ the *gradient tracking* (GT) technique that guarantees convergence of the algorithm in the presence of data heterogeneity.

Contributions. We propose the Dec-FedTrack algorithm which is a decentralized minimax optimization method over a network of n communicating nodes with two modules of local updates and gradient

tracking, and analyze its communication complexity and convergence rate for the case of nonconvex-strongly-concave (NC-SC) minimax optimization. We show that Dec-FedTrack achieves the $O(\kappa n^{-1}\epsilon^{-4})$ stochastic first-order oracle (SFO) complexity and the $O(\kappa^3\epsilon^{-2})$ communication complexity, where the condition number is defined by $\kappa \triangleq \ell/\mu$. This is the first federated minimax optimization algorithm that incorporates GT in a decentralized setting. Moreover, we conduct several numerical experiments that demonstrate the communication efficiency and adversarial robustness of Dec-FedTrack over baselines.

II. RELATED WORK

A. Federated Learning with Heterogeneous Data

One of the most challenging aspects of federated learning is data heterogeneity, where training data is not identically and independently distributed across clients (non-i.i.d.). Under such conditions, local models of clients may drift away from the global model optimum, slowing down convergence [5, 6]. Several studies have attempted to tackle this issue in federated learning [7–10]. However, these studies are typically not decentralized, their results are often limited to (strongly) convex objective functions, or they make restrictive assumptions about the gradients of objective functions. In this context, gradient tracking (GT) algorithms have been proposed to address these challenges [11–13]. Particularly, in this paper, we also leverage the GT technique to mitigate the data heterogeneity problem.

B. Decentralized Minimization

Many works have examined minimization problems within a decentralized setting [14–26]. Works such as K-GT [27], LU-GT [28] and [11, 12, 29, 30] have introduced decentralized algorithms incorporating local updates and GT, although they are tailored for minimization rather than minimax optimization.

C. Centralized Minimax Optimization

Centralized minimax optimization has become increasingly significant, particularly with the rise of machine learning applications like GANs [31] and adversarial training of neural networks. This optimization paradigm tackles the challenges posed by nonconvex-concave and nonconvex-nonconcave problems, drawing attention due to its relevance in various domains. For NC-SC problems, several works have utilized momentum or variance reduction techniques to achieve the SFO complexity of $O(\kappa^3\epsilon^{-3})$ [32–35].

D. Decentralized Minimax Optimization

Numerous studies have explored decentralized minimax optimization for (strongly) convex-concave [36–40], nonconvex-strongly-concave [41–49], and nonconvex-nonconcave [50], objective functions. DPOSG [50] has the assumption of identical distributions, and most of the mentioned works on nonconvex-strongly-concave minimax optimization have a very high gradient complexity. The closest ones to our setting and results are DM-HSGD [47], DREAM [46], and black [48]. These studies explore decentralized minimax optimization using gradient tracking and variance reduction techniques. DM-HSGD employs the variance reduction technique of STORM [51], whereas DREAM and black utilize the variance reduction technique of SPIDER [52]. However, clients in these algorithms do not perform multiple local updates between communication rounds, making them unsuitable for federated learning scenarios. Nevertheless, the best SFO complexity among these works, $O(\kappa^3\epsilon^{-3})$, is comparable to the SFO complexity of our algorithm, which is $O(\kappa n^{-1}\epsilon^{-4})$. This is due to Dec-FedTrack benefiting from linear speedup in the SFO complexity with respect to the number of clients.

E. Distributed/Federated Minimax Learning

Several works have studied minimax optimization in the federated learning setting across various function types: (strongly) convex-concave [4, 53–55] and nonconvex-strongly-concave/nonconvex-PL/nonconvex-one-point-concave [56–60]. FedGDA-GT [55] has delved into federated minimax learning with both local updates and GT, but it is not decentralized and assumes strongly-convex-strongly-concave objective functions. Momentum Local SGDA [59], SAGDA [61], and De-Norm-SGDA [60] explore federated minimax optimization with local updates but lacks decentralization and does not incorporate GT. However, Dec-FedTrack achieves an SFO complexity of $O(\kappa n^{-1}\epsilon^{-4})$, which is superior to the SFO complexity of existing methods, even in non-decentralized cases, with an SFO complexity of $O(\kappa^4 n^{-1}\epsilon^{-4})$.

We summarize the comparison of related algorithms with Dec-FedTrack in Table 1.

Table 1: Comparison of Dec-FedTrack with related algorithms for minimax and minimization optimization. Criteria in this comparison are: SFO complexity; number of communications; type of centralization; type of function class; if the algorithm is stochastic; and if the algorithm has local update (LU), heterogeneity robustness (HR), and adversarial robustness (AR).

Name	SFO	Comm. Round	Decentralized	Objective	LU	HR	AR
MLSGDA [59]	$O\left(\frac{\kappa^4}{n\epsilon^4}\right)$	$O\left(\frac{\kappa^3}{\epsilon^3}\right)$	×	NC-SC	✓	×	✓
SAGDA [61]	$O\left(\frac{\kappa^4}{n\epsilon^4}\right)$	$O\left(\frac{\kappa^2}{\epsilon^2}\right)$	×	NC-SC	✓	×	✓
Fed-Norm-SGDA [60]	$O\left(\frac{\kappa^4}{n\epsilon^4}\right)$	$O\left(\frac{\kappa^2}{\epsilon^2}\right)$	×	NC-SC	✓	×	✓
DM-HSGD [47]	$O\left(\frac{\kappa^3}{\epsilon^3}\right)$	$O\left(\frac{\kappa^3}{\epsilon^3}\right)$	✓	NC-SC	×	✓	✓
DREAM [46]	$O\left(\frac{\kappa^3}{\epsilon^3}\right)$	$O\left(\frac{\kappa^2}{\epsilon^2}\right)$	✓	NC-SC	×	✓	✓
black [48]	$O\left(\frac{\kappa^4}{\epsilon^4}\right)$	$O\left(\frac{\kappa^3}{\epsilon^2}\right)$	✓	NC-SC	×	✓	✓
K-GT [27]	$O\left(\frac{1}{n\epsilon^4}\right)$	$O\left(\frac{1}{n\epsilon^2}\right)$	✓	NC	✓	✓	×
Dec-FedTrack (Ours)	$O\left(\frac{\kappa}{n\epsilon^4}\right)$	$O\left(\frac{\kappa^3}{\epsilon^2}\right)$	✓	NC-SC	✓	✓	✓

III. PROBLEM SETUP

We consider a connected network of n clients with $\mathcal{V} = [n] := \{1, \dots, n\}$ and $\mathcal{E} \subseteq \mathcal{V} \times \mathcal{V}$ as the set of nodes and edges, respectively. This network collaboratively seeks to solve the following minimax optimization problem:

$$\min_{\mathbf{x} \in \mathbb{R}^d} \max_{\mathbf{y} \in \mathbb{R}^q} f(\mathbf{x}, \mathbf{y}) = \frac{1}{n} \sum_{i=1}^n f_i(\mathbf{x}, \mathbf{y}), \quad (1)$$

where $f_i(\mathbf{x}, \mathbf{y}) = \mathbb{E}[F_i(\mathbf{x}, \mathbf{y}; \xi^{(i)})]$ denotes the local function associated with node $i \in \mathcal{V}$. Here, the expectation is with respect to $\xi^{(i)} \sim \mathcal{D}_i$ and \mathcal{D}_i denotes the local distribution for node i . In our decentralized setting, clients communicate with each other along the edges $e \in \mathcal{E}$, that is, each node is allowed to communicate with its neighboring nodes.

A. Motivating example: Federated adversarial training

Consider a network of clients that wish to train a common model \mathbf{x} that is robust to adversarial perturbation \mathbf{y} . In this model, the adversary can attack the network by adding a common perturbation to *all* the samples of every node, i.e. *universal perturbation* [62]. This model corresponds to an adversarial cost function $f_i(\mathbf{x}, \mathbf{y})$ for each node i and results in a minimax problem shown in (1) that should be solved over the connected network. One should add that in adversarial machine learning, the adversary is restricted to a bounded noise power; therefore, in this case the minimax problem (1) will have a constraint $\|\mathbf{y}\| \leq \delta$.

B. Convergence measure

In this paper, we focus on a particular setting where each local function $f_i(\mathbf{x}, \mathbf{y})$ is nonconvex in \mathbf{x} and strongly concave in \mathbf{y} which is well-studied in the minimax optimization literature [63]. This assumption allows us to define the *primal* function of (1) for every \mathbf{x} as $\Phi(\mathbf{x}) := \max_{\mathbf{y} \in \mathbb{R}^q} f(\mathbf{x}, \mathbf{y})$. Solving the minimax problem (1) is equivalent to minimizing the primal function, i.e., $\min_{\mathbf{x} \in \mathbb{R}^d} \Phi(\mathbf{x})$ which is nonconvex. A well-established convergence measure for such minimization problems is to find a *stationary point* $\hat{\mathbf{x}}$ of Φ , that is a point for which $\|\nabla \Phi(\hat{\mathbf{x}})\| \leq \epsilon$.

C. Notation

We represent vectors using bold small letters and matrices using bold capital letters. The vector $\mathbf{x}_i^{(t)+k}$ denotes a variable on node i at local step k and communication round t , as will be explained in Section IV. The average of vectors \mathbf{x}_i is defined as $\bar{\mathbf{x}} = \frac{1}{n} \sum_i \mathbf{x}_i$. We denote a matrix whose columns are the collection of n vectors, each belonging to a client, as $\mathbf{X} \in \mathbb{R}^{d \times n}$, i.e., $\mathbf{X} = [\mathbf{x}_1, \dots, \mathbf{x}_n]$. Additionally, we use $\bar{\mathbf{X}}$ to represent a matrix whose columns are equal to $\bar{\mathbf{x}}$, and it can be written in a more useful way as

$$\bar{\mathbf{X}} = [\bar{\mathbf{x}}, \dots, \bar{\mathbf{x}}] = \frac{1}{n} \mathbf{X} \mathbf{1}_n \mathbf{1}_n^T = \mathbf{X} \mathbf{J} \in \mathbb{R}^{d \times n},$$

where $\mathbf{J} = \frac{1}{n} \mathbf{1}_n \mathbf{1}_n^T$. We also use the below notation for convenience throughout the paper:

$$\begin{aligned} \nabla F(\mathbf{X}, \mathbf{Y}; \xi) &= [\nabla F_1(\mathbf{x}_1, \mathbf{y}_1; \xi_1), \dots, \nabla F_n(\mathbf{x}_n, \mathbf{y}_n; \xi_n)], \\ \nabla f(\mathbf{X}, \mathbf{Y}) &= \mathbb{E}_{(\xi_1, \dots, \xi_n)} \nabla F(\mathbf{X}, \mathbf{Y}; \xi) = [\nabla f_1(\mathbf{x}_1, \mathbf{y}_1), \dots, \nabla f_n(\mathbf{x}_n, \mathbf{y}_n)] \in \mathbb{R}^{d \times n}. \end{aligned}$$

We denote the batch sizes for variables \mathbf{x} and \mathbf{y} as b_x and b_y , respectively. Moreover, for functions f_1, f_2 we use the notation $f_1 \lesssim f_2$ to indicate that $f_1 \leq O(f_2)$.

IV. DEC-FEDTRACK ALGORITHM

In this section, we describe our proposed method to solve the minimax problem (1) over a connected network of n nodes. Our method, namely Dec-FedTrack, comprises of two main modules: *local updates* and *gradient tracking* which we elaborate on in the following.

Dec-FedTrack (shown in Algorithm 1) consists of a number of communication rounds, T , where in each round, every node performs K local updates on its variables. In particular, in the k th iteration of round t , each node computes unbiased stochastic gradients and updates its local min and max variables \mathbf{x}_i and \mathbf{y}_i using the so-called *correction terms* (Lines 4 and 5). Next, each node obtains tracking variables

$$\begin{aligned} \mathbf{z}_i^{(t)} &= \frac{1}{K\eta_c} (\mathbf{x}_i^{(t)} - \mathbf{x}_i^{(t)+K}), \\ \mathbf{r}_i^{(t)} &= \frac{1}{K\eta_d} (\mathbf{y}_i^{(t)+K} - \mathbf{y}_i^{(t)}), \end{aligned}$$

and sends variable $\{\mathbf{z}_i^{(t)}, \mathbf{r}_i^{(t)}, \mathbf{x}_i^{(t)}, \mathbf{y}_i^{(t)}\}$ to its neighboring nodes. After aggregating these variables from the neighbors, node i updates its correction terms and model variables using gradient tracking [27] as follows:

$$\begin{aligned} \mathbf{c}_i^{(t+1)} &= \mathbf{c}_i^{(t)} - \mathbf{z}_i^{(t)} + \sum_j w_{ij} \mathbf{z}_j^{(t)}, \\ \mathbf{d}_i^{(t+1)} &= \mathbf{d}_i^{(t)} - \mathbf{r}_i^{(t)} + \sum_j w_{ij} \mathbf{r}_j^{(t)}, \\ \mathbf{x}_i^{(t+1)} &= \sum_j w_{ij} (\mathbf{x}_j^{(t)} - K\eta_x \mathbf{z}_j^{(t)}), \\ \mathbf{y}_i^{(t+1)} &= \sum_j w_{ij} (\mathbf{y}_j^{(t)} + K\eta_y \mathbf{r}_j^{(t)}), \end{aligned}$$

where $\eta_x := \eta_s \eta_c$ and $\eta_y := \eta_r \eta_d$ denote the global step sizes. The proposed Dec-FedTrack algorithm is described in Algorithm 1 using matrix notations.

Next, we comment on the necessity of using GT in our proposed algorithm. Given that clients' distributions are non-iid, to prove convergence one needs to establish an upper bound on the local gradients. While bounding assumptions can be directly imposed on local gradients, such as Assumption 3b in [64], in many distributed learning settings that are unconstrained, assuming the existence of such bounds can be restrictive. The gradient tracking algorithm [12] addresses this challenge by incorporating a correction term into gradients at each node. In fact, the correction term aims to bring the tracking variable for each client close to the tracking variable of its neighbors, preventing client-drift. The matrix format of the correction term in GT is as follows:

$$\begin{aligned} \mathbf{X}^{(t+1)} &= (\mathbf{X}^{(t)} - \eta \mathbf{Z}^{(t)}) \mathbf{W} \\ \mathbf{Z}^{(t+1)} &= \nabla F(\mathbf{X}^{(t+1)}; \xi^{(t+1)}) + \underbrace{\mathbf{Z}^{(t)} \mathbf{W} - \nabla F(\mathbf{X}^{(t)}; \xi^{(t)})}_{\text{correction term}}. \end{aligned}$$

V. CONVERGENCE ANALYSIS

In this section, we provide rigorous convergence analysis for the proposed Dec-FedTrack algorithm solving (1). The detailed proofs are provided in the appendix. Let us begin with a few assumptions.

As explained before, in our decentralized setting, agents communicate with each other along the edges of a fixed communication graph connecting n nodes. Moreover, each edge of the graph is associated with a positive mixing weight and we denote the mixing matrix by $\mathbf{W} \in \mathbb{R}^{n \times n}$.

Algorithm 1 Dec-FedTrack

Initialize: $\forall i, j \in [n], \mathbf{x}_i^{(0)} = \mathbf{x}_j^{(0)}, \mathbf{y}_i^{(0)} = \mathbf{y}_j^{(0)}; \mathbf{c}_i^{(0)}$ and $\mathbf{d}_i^{(0)}$ according to Lemma A.3.

```
1: for node  $i \in [n]$  parallel do
2:   for communication:  $t \leftarrow 0$  to  $T - 1$  do
3:     for local step:  $k \leftarrow 0$  to  $K - 1$  do
4:       Update min variables
            $\mathbf{X}^{(t)+k+1} = \mathbf{X}^{(t)+k} - \eta_c(\nabla_x F(\mathbf{X}^{(t)+k}, \mathbf{Y}^{(t)+k}; \xi^{(t)+k}) + \mathbf{C}^{(t)})$ 
5:       Update max variables
            $\mathbf{Y}^{(t)+k+1} = \mathbf{Y}^{(t)+k} + \eta_d(\nabla_y F(\mathbf{X}^{(t)+k}, \mathbf{Y}^{(t)+k}; \xi^{(t)+k}) + \mathbf{D}^{(t)})$ 
6:     end for
7:      $\mathbf{Z}^{(t)} = \frac{1}{K\eta_c} (\mathbf{X}^{(t)} - \mathbf{X}^{(t)+K})$ 
8:      $\mathbf{R}^{(t)} = \frac{1}{K\eta_d} (\mathbf{Y}^{(t)+K} - \mathbf{Y}^{(t)})$ 
9:      $\mathbf{C}^{(t+1)} = \mathbf{C}^{(t)} - \mathbf{Z}^{(t)} + \mathbf{Z}^{(t)}\mathbf{W}$ 
10:     $\mathbf{D}^{(t+1)} = \mathbf{D}^{(t)} - \mathbf{R}^{(t)} + \mathbf{R}^{(t)}\mathbf{W}$ 
11:     $\mathbf{X}^{(t+1)} = (\mathbf{X}^{(t)} - K\eta_x\mathbf{Z}^{(t)})\mathbf{W}$ 
12:     $\mathbf{Y}^{(t+1)} = (\mathbf{Y}^{(t)} + K\eta_y\mathbf{R}^{(t)})\mathbf{W}$ 
13:  end for
14: end for
```

Assumption 1: The mixing matrix \mathbf{W} has the following properties: (i) Every element of \mathbf{W} is non-negative, and $W_{i,j} = 0$ if and only if i and j are not connected, (ii) $\mathbf{W}\mathbf{1} = \mathbf{W}^\top\mathbf{1} = \mathbf{1}$, (iii) there exists a constant $0 \leq p \leq 1$ such that

$$\|\mathbf{X}\mathbf{W} - \bar{\mathbf{X}}\|_F^2 \leq (1-p)\|\mathbf{X} - \bar{\mathbf{X}}\|_F^2, \forall \mathbf{X} \in \mathbb{R}^{d \times n}.$$

The mixing rate illustrates the degree of connectivity within the network. A higher p signifies a more interconnected communication graph. When $p = 1$, $\mathbf{W} = \frac{1}{n}\mathbf{1}\mathbf{1}^\top$, suggesting full connectivity in the graph, while $p = 0$ yields $\mathbf{W} = \mathbf{I}_n$, indicating a disconnected graph [27].

Assumption 2: We assume that each local objective function f_i is ℓ -smooth, that is, for all $\mathbf{x}, \mathbf{x}', \mathbf{y}, \mathbf{y}'$

$$\|\nabla f_i(\mathbf{x}, \mathbf{y}) - \nabla f_i(\mathbf{x}', \mathbf{y}')\|^2 \leq \ell^2(\|\mathbf{x} - \mathbf{x}'\|^2 + \|\mathbf{y} - \mathbf{y}'\|^2).$$

We also assume that each $f_i(\mathbf{x}, \cdot)$ is strongly concave with respect to its second argument. We denote the condition number by $\kappa := \ell/\mu$.

The above assumption implies that the objective function f in (1) is ℓ -smooth and strongly concave with respect to its second argument.

Assumption 3: We assume that the stochastic gradients are unbiased and variance-bounded, that is,

$$\begin{aligned} \mathbb{E}[\nabla F_i(\mathbf{x}, \mathbf{y}; \xi_i)] &= \nabla f_i(\mathbf{x}, \mathbf{y}), \\ \mathbb{E}\|\nabla F_i(\mathbf{x}, \mathbf{y}; \xi_i) - \nabla f_i(\mathbf{x}, \mathbf{y})\|^2 &\leq \sigma^2. \end{aligned}$$

Assumption 4: The function $\Phi(\cdot)$ is lower bounded, that is $\inf_{\mathbf{x}} \Phi(\mathbf{x}) = \Phi^* > -\infty$.

Next, we provide the main result of the paper.

Theorem 1: Suppose Assumptions 1-4 hold and consider the iterates of Dec-FedTrack in Algorithm 1 with step-sizes $\eta_d = \Theta\left(\frac{p}{\kappa K \ell}\right)$, $\eta_c = \Theta\left(\frac{\eta_d}{\kappa^2}\right)$, and $\eta_s = \eta_r = \Theta(p)$. Then, after T communication rounds each with K local updates, there exists an iterate $0 \leq t \leq T$ such that $\mathbb{E}\|\nabla \Phi(\bar{\mathbf{x}}^{(t)})\|^2 \leq \epsilon^2$ for

$$T = O\left(\frac{\kappa^3}{p^2 \epsilon^2}\right) \mathcal{H}_0 \ell, \quad K = O\left(\frac{p^2 \sigma^2}{\kappa^2 n \epsilon^2} + \left(1 + \frac{\kappa}{\sqrt{np}}\right) \frac{\sigma}{\epsilon}\right),$$

where $\mathcal{H}_0 = O\left(1 + \frac{\delta_0}{K \kappa p}\right)$ and $\delta_0 = O\left(\frac{q}{\mu^2}\right)$.

Remark 1: Focusing on the dependency of the convergence rate on accuracy ϵ , the above theorem shows that in the regime of interest where ϵ gets small, the algorithm reaches an ϵ -stationary point within $T = O(1/\epsilon^2)$ communication rounds, each consisting of $K = O(1/\epsilon^2)$ local updates. As we elaborated in Section II

and Table 1, the proposed Dec-FedTrack algorithm simultaneously assembles all three components of local updates, heterogeneity and adversarial robustness. Apart from being theoretically provable, we will demonstrate in our numerical evaluations that these three components result in the superior performance of Dec-FedTrack over its baselines.

A. Proof Sketch

We first present the following preliminary definitions for functions with one variable:

Definition 1: A function f is called L -Lipschitz if for any \mathbf{x} and \mathbf{x}' , we have $\|f(\mathbf{x}) - f(\mathbf{x}')\| \leq L \|\mathbf{x} - \mathbf{x}'\|$.

Definition 2: A function f is called ℓ -smooth if it is differentiable and for any \mathbf{x} and \mathbf{x}' , we have $\|\nabla f(\mathbf{x}) - \nabla f(\mathbf{x}')\| \leq \ell \|\mathbf{x} - \mathbf{x}'\|$.

We then state the following standard results from optimization theory.

Proposition 1: Under Assumption 2, $\Phi(\cdot)$ is $(\ell + \kappa\ell)$ -smooth and $\mathbf{y}^*(\cdot) = \arg \max_{\mathbf{y} \in \mathbb{R}^q} f(\cdot, \mathbf{y})$ is κ -Lipschitz [32].

Proposition 2: Under Assumption 2, for every $\mathbf{x} \in \mathbb{R}^d$ and $\mathbf{y}, \mathbf{y}' \in \mathbb{R}^q$, we have

$$\nabla_{\mathbf{y}} f(\mathbf{x}, \mathbf{y})^\top (\mathbf{y} - \mathbf{y}') + \frac{1}{2\ell} \|\nabla_{\mathbf{y}} f(\mathbf{x}, \mathbf{y})\|^2 + \frac{\mu}{2} \|\mathbf{y} - \mathbf{y}'\|^2 \leq f(\mathbf{x}, \mathbf{y}^+) - f(\mathbf{x}, \mathbf{y}'),$$

where $\mathbf{y}^+ = \mathbf{y} - \frac{1}{\ell} \nabla_{\mathbf{y}} f(\mathbf{x}, \mathbf{y})$ [65].

Next, we introduce some terminology that will be useful throughout the entire proof:

1) The client (node) variance for variable \mathbf{x} that measures the deviation of variable \mathbf{x} at global steps from its averaged model:

$$\Xi_t^x := \frac{1}{n} \sum_i^n \mathbb{E} \|\mathbf{x}_i^{(t)} - \bar{\mathbf{x}}^{(t)}\|^2.$$

2) Client-drift for variable \mathbf{x} that measures the deviation of the variable \mathbf{x} at local steps from its averaged model:

$$e_{k,t}^x := \frac{1}{n} \sum_i^n \mathbb{E} \|\mathbf{x}_i^{(t)+k} - \bar{\mathbf{x}}^{(t)}\|^2.$$

The accumulation of local steps for variable \mathbf{x} is shown by

$$\mathcal{E}_t^x := \sum_{k=0}^{K-1} e_{k,t}^x = \sum_{k=0}^{K-1} \frac{1}{n} \sum_i^n \mathbb{E} \|\mathbf{x}_i^{(t)+k} - \bar{\mathbf{x}}^{(t)}\|^2.$$

3) The quality of the correction for the variable \mathbf{x} that measures the accuracy of the gradient correction in the local updates, which aims to bring local updates closer to global updates:

$$\gamma_t^x = \frac{1}{n\ell^2} \mathbb{E} \left\| \mathbf{C}^{(t)} + \nabla_{\mathbf{x}} f(\bar{\mathbf{X}}^{(t)}, \bar{\mathbf{Y}}^{(t)}) - \nabla_{\mathbf{x}} f(\bar{\mathbf{X}}^{(t)}, \bar{\mathbf{Y}}^{(t)}) \mathbf{J} \right\|_F^2.$$

Similarly, we can define $\Xi_t^y, e_{k,t}^y, \mathcal{E}_t^y$, and γ_t^y for variable \mathbf{y} .

4) Consensus distance for variable \mathbf{y} that measures the deviation of the optimum \mathbf{y} when $\mathbf{x} = \bar{\mathbf{x}}$ and the averaged \mathbf{y} , that is, $\delta_t = \|\hat{\mathbf{y}}^{(t)} - \bar{\mathbf{y}}^{(t)}\|^2$ where $\hat{\mathbf{y}}^{(t)} = \arg \max_{\mathbf{y} \in \mathbb{R}^q} f(\bar{\mathbf{x}}^{(t)}, \mathbf{y})$.

Next, we provide recursion bounds for client variance, client drift, and quality of correction—for both variables \mathbf{x} and \mathbf{y} —as well as consensus distance for variable \mathbf{y} .

Lemma 1: Under the assumption that $\eta_c, \eta_d \lesssim \frac{1}{KL}$, we can bound the local drift for variables \mathbf{x} and \mathbf{y} as

$$\begin{aligned} \mathcal{E}_t^x &\lesssim K\Xi_t^x + K^2\eta_c^2\ell^2\mathcal{E}_t^y + K^3\eta_c^2\ell^2\gamma_t^x + K^3\eta_c^2\ell^2\delta_t + K^3\eta_c^2\mathbb{E} \left\| \nabla \Phi(\bar{\mathbf{x}}^{(t)}) \right\|^2 + K^2\eta_c^2\sigma^2, \\ \mathcal{E}_t^y &\lesssim K\Xi_t^y + K^2\eta_d^2\ell^2\mathcal{E}_t^x + K^3\eta_d^2\ell^2\gamma_t^y + K^3\eta_d^2\ell^2\delta_t + K^2\eta_d^2\sigma^2. \end{aligned}$$

Lemma 2: We have the following bounds on client variance for variable \mathbf{x} and \mathbf{y}

$$\begin{aligned} \Xi_{t+1}^x &\lesssim \left(1 - \frac{p}{2}\right) \Xi_t^x + \frac{K\eta_x^2\ell^2}{p} (\mathcal{E}_t^x + \mathcal{E}_t^y) + \frac{K^2\eta_x^2\ell^2}{p} \gamma_t^x + K\eta_x^2\sigma^2, \\ \Xi_{t+1}^y &\lesssim \left(1 - \frac{p}{2}\right) \Xi_t^y + \frac{K\eta_y^2\ell^2}{p} (\mathcal{E}_t^x + \mathcal{E}_t^y) + \frac{K^2\eta_y^2\ell^2}{p} \gamma_t^y + K\eta_y^2\sigma^2. \end{aligned}$$

Lemma 3: Assuming that $\eta_x, \eta_y \lesssim \frac{\sqrt{p}}{K\ell}$, we have the following bounds on the quality of correction for variables \mathbf{x} and \mathbf{y}

$$\begin{aligned}\gamma_{t+1}^x &\lesssim \left(1 - \frac{p}{2}\right) \gamma_t^x + \frac{1}{pK} (\mathcal{E}_t^x + \mathcal{E}_t^y) + \frac{K^2 \ell^2}{p} (2\eta_x^2 + \eta_y^2) \delta_t + \frac{K^2 \eta_x^2}{p} \mathbb{E} \left\| \nabla \Phi \left(\bar{\mathbf{x}}^{(t)} \right) \right\|^2 + \frac{\sigma^2}{K\ell^2}, \\ \gamma_{t+1}^y &\lesssim \left(1 - \frac{p}{2}\right) \gamma_t^y + \frac{1}{pK} (\mathcal{E}_t^x + \mathcal{E}_t^y) + \frac{K^2 \ell^2}{p} (2\eta_x^2 + \eta_y^2) \delta_t + \frac{K^2 \eta_x^2}{p} \mathbb{E} \left\| \nabla \Phi \left(\bar{\mathbf{x}}^{(t)} \right) \right\|^2 + \frac{\sigma^2}{K\ell^2}.\end{aligned}$$

Lemma 4: Assuming that $\eta_x \lesssim \frac{\eta_y}{\kappa^2}$ and $\eta_y \leq \frac{1}{K\ell}$, we have the following bound on δ_t

$$\delta_{t+1} \lesssim \left(1 - \frac{K\eta_y \ell}{\kappa}\right) \delta_t + \eta_y \ell \kappa (\mathcal{E}_t^x + \mathcal{E}_t^y) + \frac{\kappa^3 K \eta_x^2}{\eta_y \ell} \mathbb{E} \left\| \nabla \Phi \left(\bar{\mathbf{x}}^{(t)} \right) \right\|^2 + \frac{\eta_y \sigma^2 \kappa}{n\ell}.$$

Now, we state the following descent lemma for $\Phi(\mathbf{x})$:

Lemma 5: Assuming that $\eta_x \lesssim \frac{1}{K\ell\kappa}$, we have the following bound on $\mathbb{E}\Phi(\bar{\mathbf{x}}^{(t+1)})$ as follows:

$$\mathbb{E}\Phi(\bar{\mathbf{x}}^{(t+1)}) \lesssim \mathbb{E}\Phi(\bar{\mathbf{x}}^{(t)}) + \eta_x \ell^2 (\mathcal{E}_t^x + \mathcal{E}_t^y) + \ell^2 \eta_x K \delta_t - \eta_x K \mathbb{E} \left\| \nabla \Phi \left(\bar{\mathbf{x}}^{(t)} \right) \right\|^2 + \frac{K \eta_x^2 \ell \sigma^2 \kappa}{n}.$$

Using Lemmas 1-5, we have the following recursive bound on the Lyapunov function \mathcal{H}_t .

Lemma 6: Under the assumption that $\eta_d = \Theta\left(\frac{p}{\kappa K\ell}\right)$, $\eta_c = \Theta\left(\frac{\eta_d}{\kappa^2}\right)$, and $\eta_s = \eta_r = \Theta(p)$, we can find constants A_x, A_y, B_x, B_y , and C , such that

$$\mathcal{H}_{t+1} - \mathcal{H}_t \lesssim -K\eta_x \mathbb{E} \left\| \nabla \Phi \left(\bar{\mathbf{x}}^{(t)} \right) \right\|^2 + \frac{1}{p} K \ell \eta_d^3 \sigma^2 + \frac{K \eta_x^2 \ell \kappa}{n} \sigma^2 + \frac{\eta_y}{n\ell K p} \sigma^2,$$

where

$$\mathcal{H}_t = \mathbb{E}\Phi(\bar{\mathbf{x}}^{(t)}) - \mathbb{E}\Phi(\mathbf{x}^*) + A_x \eta_d \ell \Xi_t^x + A_y \eta_d \ell \Xi_t^y + B_x K^2 \ell^3 \eta_d^3 \gamma_t^x + B_y K^2 \ell^3 \eta_d^3 \gamma_t^y + C \frac{1}{K\kappa p} \delta_t.$$

Using the telescopic sum for \mathcal{H}_t , we have

$$\begin{aligned}\frac{1}{T+1} \sum_{t=0}^T (\mathcal{H}_{t+1} - \mathcal{H}_t) &= \frac{1}{T+1} (\mathcal{H}_{T+1} - \mathcal{H}_0) \\ &\lesssim -K\eta_x \frac{1}{T+1} \sum_{t=0}^T \mathbb{E} \left\| \nabla \Phi \left(\bar{\mathbf{x}}^{(t)} \right) \right\|^2 + \frac{1}{p} K \ell \eta_d^3 \sigma^2 + \frac{K \eta_x^2 \ell \kappa}{n} \sigma^2 + \frac{\eta_y}{n\ell K p} \sigma^2,\end{aligned}$$

which results in

$$\frac{1}{T+1} \sum_{t=0}^T \mathbb{E} \left\| \nabla \Phi \left(\bar{\mathbf{x}}^{(t)} \right) \right\|^2 \lesssim \frac{\mathcal{H}_0 - \mathcal{H}_{T+1}}{(T+1) K \eta_x} + \frac{\ell \eta_d^3}{p \eta_x} \sigma^2 + \frac{\eta_x \ell \kappa}{n} \sigma^2 + \frac{\eta_y}{n\ell K^2 p \eta_x}. \quad (2)$$

Now, we want to ensure $\frac{1}{T+1} \sum_{t=0}^T \mathbb{E} \left\| \nabla \Phi \left(\bar{\mathbf{x}}^{(t)} \right) \right\|^2 \leq \epsilon^2$ for any arbitrary $\epsilon > 0$, which is equivalent to aligning each term on the RHS of (2) to the order of ϵ^2 . Given that $\eta_x = \Theta\left(\frac{p^2}{\kappa^3 K\ell}\right)$, and $\eta_y = \Theta\left(\frac{p^2}{\kappa K\ell}\right)$, we can conclude that $T = O\left(\frac{\kappa^3}{p^2 \epsilon^2}\right) \mathcal{H}_0 \ell$, $K = O\left(\frac{p^2 \sigma^2}{\kappa^2 n \epsilon^2} + \left(1 + \frac{\kappa}{\sqrt{np}}\right) \frac{\sigma}{\epsilon}\right)$.

VI. NUMERICAL RESULTS

A. Robust Logistic Regression

We consider the problem of training a robust logistic regression classifier with a non-convex regularizer similar to [47]. In this problem, we aim to train a binary classifier $\mathbf{x} \in \mathbb{R}^d$ on the a9a dataset $\{(a_k, b_k)\}_{k=1}^{mn}$, where $a_k \in \mathbb{R}^d$ denotes the feature vector and $b_k \in \{-1, +1\}$ represents the label for the k -th sample in the dataset [66]. Each client or node is allocated m samples, resulting in a total of $N = mn$ samples. The loss function at each client is given by

$$f_i(\mathbf{x}, \mathbf{y}) = \frac{1}{m} \sum_{j=1}^m (l_{ij} - V(\mathbf{y}) + g(\mathbf{x})),$$

where $l_{ij} = \log\left(1 + \exp\left(-b_{ij} (a_{ij} + \mathbf{y})^\top \mathbf{x}\right)\right)$ denotes the logistic loss, $V(\mathbf{y}) = \frac{\lambda_1}{2} \|\mathbf{y}\|^2$ is a soft penalty term to bound the norm of the perturbation \mathbf{y} , and $g(x) = \lambda_2 \sum_{i=1}^d \frac{\alpha x_i^2}{1 + \alpha x_i^2}$ is a non-convex regularizer. We generate a network using a connected Erdos-Renyi graph with an edge probability of p_c . The mixing

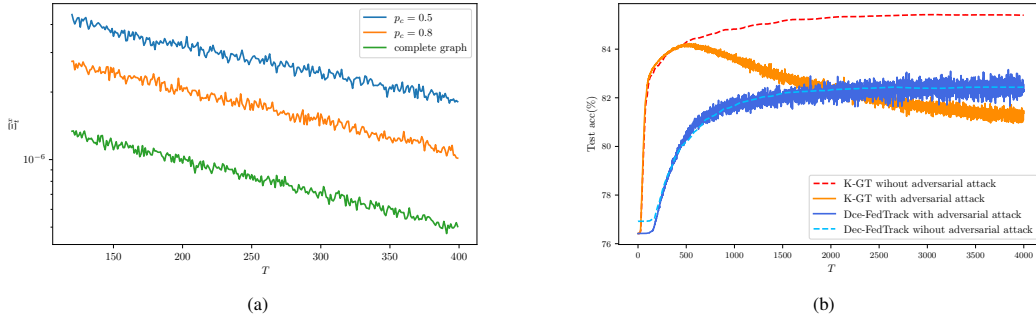


Fig. 1: (a) Empirical client variance for the variable \mathbf{x} (Ξ_t^x) versus the number of communication rounds for different values of graph connectivity ratio: $p_c \in \{0.5, 0.8\}$, and complete graph. (b) Test accuracy versus the communication rounds with and without adversarial noise for K-GT and Fed-GradTrack algorithms.

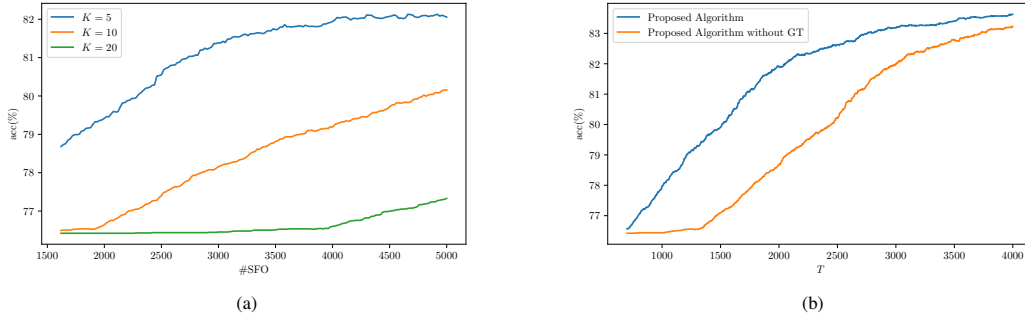


Fig. 2: (a) The accuracy of test data versus the number of stochastic first-order oracle (SFO) uses for different amounts of local updates: $K \in \{5, 10, 20\}$. (b) The accuracy of test data versus the communication rounds for both the proposed algorithm and proposed algorithm without GT.

matrix of the network is then set to $\mathbf{W} = \mathbf{I} - \frac{2}{3\lambda_{\max}(\mathbf{L})}\mathbf{L}$, where \mathbf{L} is the Laplacian matrix of the graph network with the largest eigenvalue $\lambda_{\max}(\mathbf{L})$.

First, we demonstrate the impact of network connectivity on $\Xi_t^x := \frac{1}{n} \sum_i^n \mathbb{E} \|\mathbf{x}_i^{(t)} - \bar{\mathbf{x}}^{(t)}\|^2$, representing the client variance for the variable \mathbf{x} . Fig. 1a illustrates this effect for $p_c = 0.5$, $p_c = 0.8$, and a complete graph. We employed parameters $\lambda_1 = 1$, $\lambda_2 = 10^{-3}$, $\alpha = 10$, $K = 20$, $T = 400$, $b_x = b_y = 20$, $n = 10$, $\eta_c = 0.0002$, $\eta_d = 0.001$, $\eta_s = \eta_r = 1$ and the dataset a9a, where $a_k \in \mathbb{R}^{123}$. As it can be seen, larger graph connectivity leads to smaller client variance and faster convergence.

In Figure 1b, we show the *test accuracy* of the learned model versus the number of communication rounds with and without adversarial noise for Dec-FedTrack and K-GT, a benchmark minimization algorithm for our setting. We employed parameters $\eta_c = 0.01$ for K-GT, and $\eta_c = 0.002$ and $\eta_d = 0.01$ for Dec-FedTrack algorithms. Moreover, we set $p_c = 0.8$, $K = 5$, and $T = 4000$ for both algorithms and maintained the remaining parameters similar to those in Fig. 1a. We also added projected gradient descent (PGD) adversarial noise (δ) with $\delta = 0.1$, 30 iterations, and a step size of $\eta = 0.1$ to the test data before computing the accuracy. As illustrated, K-GT exhibits slightly better performance than Dec-FedTrack without adversarial noise; However, with adversarial noise, Dec-FedTrack demonstrates greater robustness.

Fig. 2a illustrates the effect of local updates on the test accuracy for three different values of K . For $K \in \{5, 10, 20\}$ we used $\eta_c \in \{0.004, 0.002, 0.001\}$ and $\eta_d \in \{0.02, 0.01, 0.005\}$, respectively. We set $p_c = 0.5$ and kept the remaining parameters similar to those in Fig. 1a. As it is expected, there is a tradeoff between speed of convergence and communication efficiency. We observe that when K is larger, i.e. we have more local updates, the sample complexity to achieve the same accuracy becomes larger.

Fig. 2b illustrates the effect of GT in the proposed algorithm when clients have non-iid sample distribution. We used parameters $b_x = b_y = 100$, $p_c = 0.5$, $T = 4000$, and other parameters similar to those in Fig. 1a. We observe that GT enables faster convergence of the decentralized minimax optimization algorithm

Table 2: Model architecture for the CNN. We used convolutional layer (Conv2D), max pooling layer (MaxPool2D), and fully connected layer.

layer	details
1	Conv2D(1, 16, 5, 1, 2), MaxPool2D(2), ReLU
2	Conv2D(16, 32, 5, 1, 2), MaxPool2D(2), ReLU
3	FC($32 \times 7 \times 7$, 50), ReLU
4	FC(50,10)

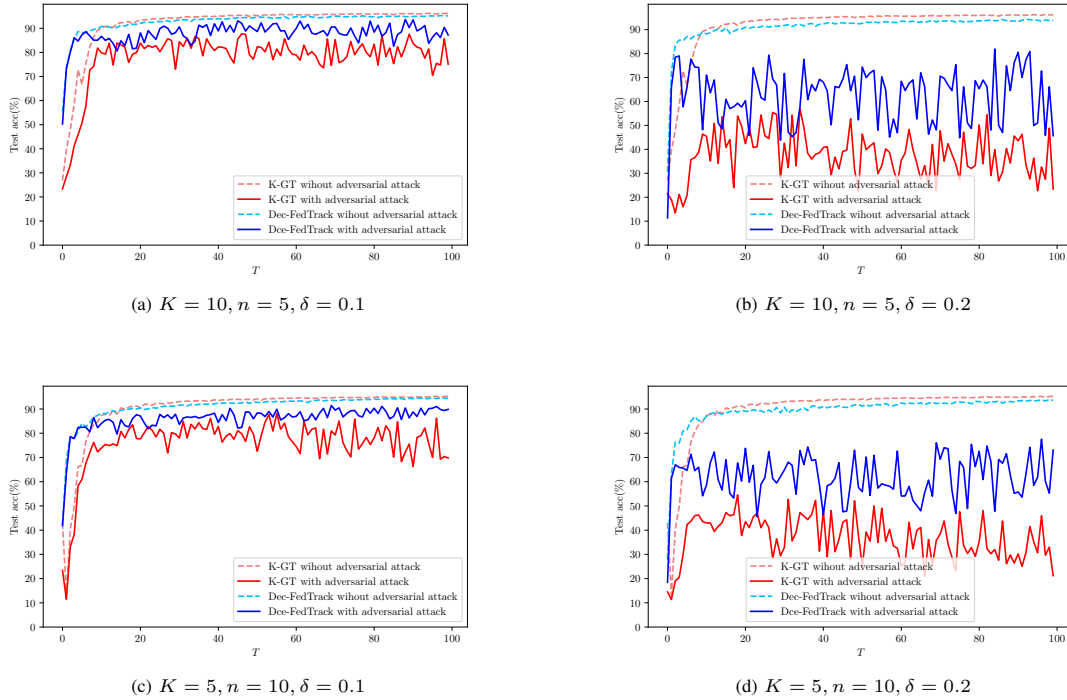


Fig. 3: Test accuracy versus the number of communication rounds for different K , n , and δ for DNN. In (b) and (d) adversarial noise is higher so the test accuracy is lower than (a) and (c), but in all figures Dec-FedTrack is more robust than K-GT.

as higher accuracy can be achieved by employing GT with fewer rounds of communication.

B. Robust Neural Network Training

We conducted experiments using the MNIST dataset, comprising 60,000 images of size 28×28 , each labeled with one of 10 categories. Our study involves two neural network architectures: a 2-layer deep neural network (DNN) and a convolutional neural network (CNN).

For the 2-layer DNN, we employed two fully connected layers with 50 and 10 neurons, respectively. Details of the CNN architecture are provided in Table 2.

We initially evaluated the robustness of Dec-FedTrack against adversarial attacks, comparing it with K-GT, a benchmark minimization algorithm. We trained both the DNN and CNN using K-GT and Dec-FedTrack with varying values of $n \in \{5, 10\}$, $K \in \{5, 10\}$, and explored different constant learning rates within $\{1, 0.5, 0.1, 0.05, 0.01\}$. Additionally, we set $p_c = 0.7$ and $b_x = b_y = 128$. For adversarial attacks, we employed the PGD method with 20 iterations, a step size of $\eta = 0.1$, and δ values from the set $\{0.1, 0.2\}$.

Figure 3 illustrates the test accuracy versus communication rounds for the DNN. Notably, while K-GT shows marginally better accuracy than Dec-FedTrack in the absence of adversarial attacks, the latter demonstrates significantly enhanced robustness when subjected to adversarial perturbations.

In Figure 4, we present the test accuracy for $K = n = 5$, and $\delta \in \{0.1, 0.2\}$ for the DNN and $\delta \in \{0.2, 0.3\}$ for the CNN. Our results indicate that the CNN architecture exhibits greater robustness against adversarial attacks compared to the DNN. However, in all cases Dec-FedTrack consistently outperforms K-GT.

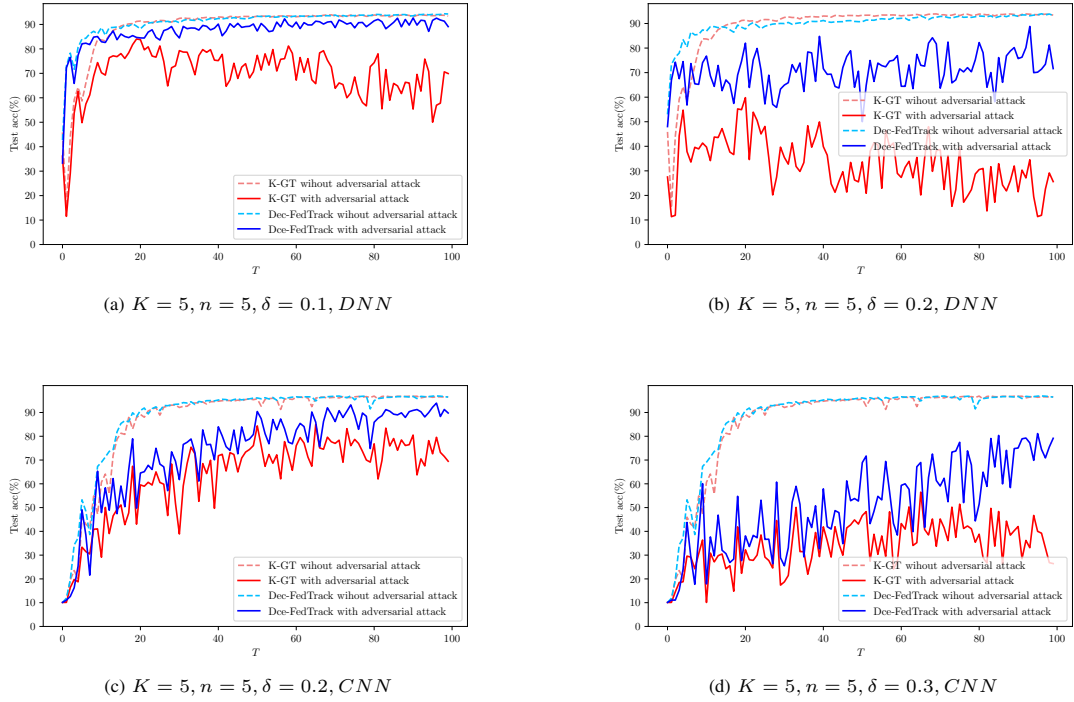


Fig. 4: Test accuracy versus the number of communication rounds for $K = n = 5$, and $\delta \in \{0.2, 0.3\}$ for DNN and CNN.

VII. CONCLUSION

This paper presents Dec-FedTrack, a decentralized minimax optimization algorithm specifically tailored for addressing the challenges prevalent in distributed learning systems, particularly within federated learning setups. Dec-FedTrack, by integrating local updates and gradient tracking mechanisms, aims to enhance robustness against universal adversarial perturbations while efficiently mitigating data heterogeneity. The theoretical analysis establishes convergence guarantees under certain assumptions, affirming Dec-FedTrack's reliability and efficacy. Our empirical evaluations demonstrate that for an equal adversary budget, Dec-FedTrack is more robust to adversarial perturbations compared to non-robust baselines such as K-GT.

REFERENCES

- [1] J. Konečný, H. B. McMahan, F. X. Yu, P. Richtárik, A. T. Suresh, and D. Bacon, “Federated learning: Strategies for improving communication efficiency,” *arXiv preprint arXiv:1610.05492*, 2016.
- [2] P. Kairouz, H. B. McMahan, B. Avent, A. Bellet, M. Bennis, A. N. Bhagoji, K. Bonawitz, Z. Charles, G. Cormode, R. Cummings *et al.*, “Advances and open problems in federated learning,” *Foundations and Trends® in Machine Learning*, vol. 14, no. 1–2, pp. 1–210, 2021.
- [3] F. Farnia, A. Reisizadeh, R. Pedarsani, and A. Jadbabaie, “An optimal transport approach to personalized federated learning,” *IEEE Journal on Selected Areas in Information Theory*, vol. 3, no. 2, pp. 162–171, 2022.
- [4] A. Reisizadeh, F. Farnia, R. Pedarsani, and A. Jadbabaie, “Robust federated learning: The case of affine distribution shifts,” *Advances in Neural Information Processing Systems*, vol. 33, pp. 21 554–21 565, 2020.
- [5] K. Hsieh, A. Phanishayee, O. Mutlu, and P. Gibbons, “The non-iid data quagmire of decentralized machine learning,” in *International Conference on Machine Learning*. PMLR, 2020, pp. 4387–4398.
- [6] T. Li, A. K. Sahu, M. Zaheer, M. Sanjabi, A. Talwalkar, and V. Smith, “Federated optimization in heterogeneous networks,” *Proceedings of Machine learning and systems*, vol. 2, pp. 429–450, 2020.
- [7] G. Zhou, Q. Li, Y. Liu, Y. Zhao, Q. Tan, S. Yao, and K. Xu, “Fedpage: Pruning adaptively toward global efficiency of heterogeneous federated learning,” *IEEE/ACM Transactions on Networking*, 2023.
- [8] A. Rodio, F. Faticanti, O. Marfoq, G. Neglia, and E. Leonardi, “Federated learning under heterogeneous and correlated client availability,” *IEEE/ACM Transactions on Networking*, 2023.
- [9] L. Wang, Y. Xu, H. Xu, Z. Jiang, M. Chen, W. Zhang, and C. Qian, “Bose: Block-wise federated learning in heterogeneous edge computing,” *IEEE/ACM Transactions on Networking*, 2023.
- [10] J. Liu, S. Wang, H. Xu, Y. Xu, Y. Liao, J. Huang, and H. Huang, “Federated learning with experience-driven model migration in heterogeneous edge networks,” *IEEE/ACM Transactions on Networking*, 2024.
- [11] A. Koloskova, T. Lin, and S. U. Stich, “An improved analysis of gradient tracking for decentralized machine learning,” *Advances in Neural Information Processing Systems*, vol. 34, pp. 11 422–11 435, 2021.
- [12] S. Pu and A. Nedić, “Distributed stochastic gradient tracking methods,” *Mathematical Programming*, vol. 187, pp. 409–457, 2021.
- [13] J. Zhang and K. You, “Decentralized stochastic gradient tracking for non-convex empirical risk minimization,” *arXiv preprint arXiv:1909.02712*, 2019.
- [14] C. Chen, J. Zhang, L. Shen, P. Zhao, and Z. Luo, “Communication efficient primal-dual algorithm for nonconvex nonsmooth distributed optimization,” in *International Conference on Artificial Intelligence and Statistics*. PMLR, 2021, pp. 1594–1602.
- [15] H. Hendrikx, F. Bach, and L. Massoulié, “An optimal algorithm for decentralized finite-sum optimization,” *SIAM Journal on Optimization*, vol. 31, no. 4, pp. 2753–2783, 2021.
- [16] D. Kovalev, A. Salim, and P. Richtárik, “Optimal and practical algorithms for smooth and strongly convex decentralized optimization,” *Advances in Neural Information Processing Systems*, vol. 33, pp. 18 342–18 352, 2020.
- [17] B. Li, S. Cen, Y. Chen, and Y. Chi, “Communication-efficient distributed optimization in networks with gradient tracking and variance reduction,” *Journal of Machine Learning Research*, vol. 21, no. 180, pp. 1–51, 2020.
- [18] B. Li, Z. Li, and Y. Chi, “Destress: Computation-optimal and communication-efficient decentralized nonconvex finite-sum optimization,” *SIAM Journal on Mathematics of Data Science*, vol. 4, no. 3, pp. 1031–1051, 2022.

- [19] H. Li, Z. Lin, and Y. Fang, “Variance reduced extra and digging and their optimal acceleration for strongly convex decentralized optimization,” *Journal of Machine Learning Research*, vol. 23, no. 222, pp. 1–41, 2022.
- [20] W. Shi, Q. Ling, G. Wu, and W. Yin, “Extra: An exact first-order algorithm for decentralized consensus optimization,” *SIAM Journal on Optimization*, vol. 25, no. 2, pp. 944–966, 2015.
- [21] H. Sun, S. Lu, and M. Hong, “Improving the sample and communication complexity for decentralized non-convex optimization: Joint gradient estimation and tracking,” in *International conference on machine learning*. PMLR, 2020, pp. 9217–9228.
- [22] C. A. Uribe, S. Lee, A. Gasnikov, and A. Nedić, “A dual approach for optimal algorithms in distributed optimization over networks,” in *2020 Information Theory and Applications Workshop (ITA)*. IEEE, 2020, pp. 1–37.
- [23] Z. Wang, J. Zhang, T.-H. Chang, J. Li, and Z.-Q. Luo, “Distributed stochastic consensus optimization with momentum for nonconvex nonsmooth problems,” *IEEE Transactions on Signal Processing*, vol. 69, pp. 4486–4501, 2021.
- [24] R. Xin, U. A. Khan, and S. Kar, “Fast decentralized nonconvex finite-sum optimization with recursive variance reduction,” *SIAM Journal on Optimization*, vol. 32, no. 1, pp. 1–28, 2022.
- [25] K. Yuan, Q. Ling, and W. Yin, “On the convergence of decentralized gradient descent,” *SIAM Journal on Optimization*, vol. 26, no. 3, pp. 1835–1854, 2016.
- [26] J. Liu, J. Liu, H. Xu, Y. Liao, Z. Wang, and Q. Ma, “Yoga: Adaptive layer-wise model aggregation for decentralized federated learning,” *IEEE/ACM Transactions on Networking*, 2023.
- [27] Y. Liu, T. Lin, A. Koloskova, and S. U. Stich, “Decentralized gradient tracking with local steps,” 2023.
- [28] E. D. H. Nguyen, S. A. Alghunaim, K. Yuan, and C. A. Uribe, “On the performance of gradient tracking with local updates,” 2022.
- [29] F. Haddadpour, M. M. Kamani, A. Mokhtari, and M. Mahdavi, “Federated learning with compression: Unified analysis and sharp guarantees,” in *International Conference on Artificial Intelligence and Statistics*. PMLR, 2021, pp. 2350–2358.
- [30] A. S. Berahas, R. Bollapragada, and S. Gupta, “Balancing communication and computation in gradient tracking algorithms for decentralized optimization,” *arXiv preprint arXiv:2303.14289*, 2023.
- [31] I. Goodfellow, J. Pouget-Abadie, M. Mirza, B. Xu, D. Warde-Farley, S. Ozair, A. Courville, and Y. Bengio, “Generative adversarial nets,” *Advances in neural information processing systems*, vol. 27, 2014.
- [32] T. Lin, C. Jin, and M. Jordan, “On gradient descent ascent for nonconvex-concave minimax problems,” in *International Conference on Machine Learning*. PMLR, 2020, pp. 6083–6093.
- [33] S. Qiu, Z. Yang, X. Wei, J. Ye, and Z. Wang, “Single-timescale stochastic nonconvex-concave optimization for smooth nonlinear td learning,” *arXiv preprint arXiv:2008.10103*, 2020.
- [34] L. Luo, H. Ye, Z. Huang, and T. Zhang, “Stochastic recursive gradient descent ascent for stochastic nonconvex-strongly-concave minimax problems,” *Advances in Neural Information Processing Systems*, vol. 33, pp. 20 566–20 577, 2020.
- [35] S. Zhang, J. Yang, C. Guzmán, N. Kiyavash, and N. He, “The complexity of nonconvex-strongly-concave minimax optimization,” in *Uncertainty in Artificial Intelligence*. PMLR, 2021, pp. 482–492.
- [36] A. Koppel, F. Y. Jakubiec, and A. Ribeiro, “A saddle point algorithm for networked online convex optimization,” *IEEE Transactions on Signal Processing*, vol. 63, no. 19, pp. 5149–5164, 2015.
- [37] D. Mateos-Núñez and J. Cortés, “Distributed subgradient methods for saddle-point problems,” in *2015 54th IEEE Conference on Decision and Control (CDC)*. IEEE, 2015, pp. 5462–5467.

- [38] A. Rogozin, A. Beznosikov, D. Dvinskikh, D. Kovalev, P. Dvurechensky, and A. Gasnikov, “Decentralized saddle point problems via non-euclidean mirror prox,” *Optimization Methods and Software*, pp. 1–26, 2024.
- [39] A. Beznosikov, G. Scutari, A. Rogozin, and A. Gasnikov, “Distributed saddle-point problems under data similarity,” *Advances in Neural Information Processing Systems*, vol. 34, pp. 8172–8184, 2021.
- [40] A. Beznosikov, A. Rogozin, D. Kovalev, and A. Gasnikov, “Near-optimal decentralized algorithms for saddle point problems over time-varying networks,” in *Optimization and Applications: 12th International Conference, OPTIMA 2021, Petrovac, Montenegro, September 27–October 1, 2021, Proceedings 12*. Springer, 2021, pp. 246–257.
- [41] X. Wu, Z. Hu, and H. Huang, “Decentralized riemannian algorithm for nonconvex minimax problems,” *arXiv preprint arXiv:2302.03825*, 2023.
- [42] Z. Liu, X. Zhang, S. Lu, and J. Liu, “Precision: Decentralized constrained min-max learning with low communication and sample complexities,” *arXiv preprint arXiv:2303.02532*, 2023.
- [43] Y. Xu, “Decentralized gradient descent maximization method for composite nonconvex strongly-concave minimax problems,” *arXiv preprint arXiv:2304.02441*, 2023.
- [44] H. Gao, “Decentralized stochastic gradient descent ascent for finite-sum minimax problems,” *arXiv preprint arXiv:2212.02724*, 2022.
- [45] G. Mancino-Ball and Y. Xu, “Variance-reduced accelerated methods for decentralized stochastic double-regularized nonconvex strongly-concave minimax problems,” *arXiv preprint arXiv:2307.07113*, 2023.
- [46] L. Chen, H. Ye, and L. Luo, “A simple and efficient stochastic algorithm for decentralized nonconvex-strongly-concave minimax optimization,” *arXiv preprint arXiv:2212.02387*, 2022.
- [47] W. Xian, F. Huang, Y. Zhang, and H. Huang, “A faster decentralized algorithm for nonconvex minimax problems,” *Advances in Neural Information Processing Systems*, vol. 34, pp. 25 865–25 877, 2021.
- [48] X. Zhang, G. Mancino-Ball, N. S. Aybat, and Y. Xu, “Jointly improving the sample and communication complexities in decentralized stochastic minimax optimization,” *arXiv preprint arXiv:2307.09421*, 2023.
- [49] I. Tsaknakis, M. Hong, and S. Liu, “Decentralized min-max optimization: Formulations, algorithms and applications in network poisoning attack,” in *ICASSP 2020-2020 IEEE International Conference on Acoustics, Speech and Signal Processing (ICASSP)*. IEEE, 2020, pp. 5755–5759.
- [50] M. Liu, W. Zhang, Y. Mroueh, X. Cui, J. Ross, T. Yang, and P. Das, “A decentralized parallel algorithm for training generative adversarial nets,” *Advances in Neural Information Processing Systems*, vol. 33, pp. 11 056–11 070, 2020.
- [51] A. Cutkosky and F. Orabona, “Momentum-based variance reduction in non-convex sgd,” *Advances in neural information processing systems*, vol. 32, 2019.
- [52] C. Fang, C. J. Li, Z. Lin, and T. Zhang, “Spider: Near-optimal non-convex optimization via stochastic path-integrated differential estimator,” *Advances in neural information processing systems*, vol. 31, 2018.
- [53] C. Hou, K. K. Thekumparampil, G. Fanti, and S. Oh, “Efficient algorithms for federated saddle point optimization,” *arXiv preprint arXiv:2102.06333*, 2021.
- [54] L. Liao, L. Shen, J. Duan, M. Kolar, and D. Tao, “Local adagrad-type algorithm for stochastic convex-concave minimax problems,” *arXiv preprint arXiv:2106.10022*, 2021.
- [55] Z. Sun and E. Wei, “A communication-efficient algorithm with linear convergence for federated minimax learning,” *Advances in Neural Information Processing Systems*, vol. 35, pp. 6060–6073, 2022.

- [56] Y. Deng, M. M. Kamani, and M. Mahdavi, “Distributionally robust federated averaging,” *Advances in neural information processing systems*, vol. 33, pp. 15 111–15 122, 2020.
- [57] Y. Deng and M. Mahdavi, “Local stochastic gradient descent ascent: Convergence analysis and communication efficiency,” in *International Conference on Artificial Intelligence and Statistics*. PMLR, 2021, pp. 1387–1395.
- [58] J. Xie, C. Zhang, Y. Zhang, Z. Shen, and H. Qian, “A federated learning framework for nonconvex-pl minimax problems,” *arXiv preprint arXiv:2105.14216*, 2021.
- [59] P. Sharma, R. Panda, G. Joshi, and P. Varshney, “Federated minimax optimization: Improved convergence analyses and algorithms,” in *International Conference on Machine Learning*. PMLR, 2022, pp. 19 683–19 730.
- [60] P. Sharma, R. Panda, and G. Joshi, “Federated minimax optimization with client heterogeneity,” *arXiv preprint arXiv:2302.04249*, 2023.
- [61] H. Yang, X. Zhang, Z. Liu, and J. Liu, “Sagda: achieving $\mathcal{O}(\epsilon^{-2})$ communication complexity in federated min-max learning,” in *Proceedings of the 36th International Conference on Neural Information Processing Systems*, 2022, pp. 7142–7154.
- [62] S.-M. Moosavi-Dezfooli, A. Fawzi, O. Fawzi, and P. Frossard, “Universal adversarial perturbations,” in *Proceedings of the IEEE conference on computer vision and pattern recognition*, 2017, pp. 1765–1773.
- [63] T. Lin, C. Jin, and M. I. Jordan, “Near-optimal algorithms for minimax optimization,” in *Conference on Learning Theory*. PMLR, 2020, pp. 2738–2779.
- [64] A. Koloskova, N. Loizou, S. Boreiri, M. Jaggi, and S. Stich, “A unified theory of decentralized sgd with changing topology and local updates,” in *International Conference on Machine Learning*. PMLR, 2020, pp. 5381–5393.
- [65] S. Bubeck *et al.*, “Convex optimization: Algorithms and complexity,” *Foundations and Trends® in Machine Learning*, vol. 8, no. 3-4, pp. 231–357, 2015.
- [66] J. C. Platt, “12 fast training of support vector machines using sequential minimal optimization,” *Advances in kernel methods*, pp. 185–208, 1999.

APPENDIX

Lemma A.1: For a set of arbitrary vectors a_1, \dots, a_n such that $a_i \in \mathbb{R}^d$, we have

$$\left\| \frac{1}{n} \sum_{i=1}^n a_i \right\|^2 \leq \frac{1}{n} \sum_{i=1}^n \|a_i\|^2.$$

Lemma A.2: (Young's Inequality) For any vectors $a, b \in \mathbb{R}^d$ and $\alpha > 0$ we have

$$\begin{aligned} 2\langle a, b \rangle &\leq \alpha \|a\|^2 + \frac{1}{\alpha} \|b\|^2, \\ \|a + b\|^2 &\leq (1 + \alpha) \|a\|^2 + \left(1 + \frac{1}{\alpha}\right) \|b\|^2. \end{aligned}$$

Lemma A.3: If we initialize $\mathbf{C}^{(0)}$ and $\mathbf{D}^{(0)}$ as below

$$\begin{aligned} \mathbf{c}_i^{(0)} &= -\nabla_x F_i(\mathbf{x}^{(0)}, \mathbf{y}^{(0)}; \xi_i) + \frac{1}{n} \sum_j \nabla_x F_j(\mathbf{x}^{(0)}, \mathbf{y}^{(0)}; \xi_j), \\ \mathbf{d}_i^{(0)} &= -\nabla_y F_i(\mathbf{x}^{(0)}, \mathbf{y}^{(0)}; \xi_i) + \frac{1}{n} \sum_j \nabla_y F_j(\mathbf{x}^{(0)}, \mathbf{y}^{(0)}; \xi_j), \end{aligned} \quad (3)$$

then the averaged correction for variables \mathbf{x} and \mathbf{y} in any communication round equals to zero.

Proof. According to Algorithm 1 we have

$$\mathbf{C}^{(t+1)} \mathbf{J} = \mathbf{C}^{(t)} \mathbf{J} + \frac{1}{K\eta_c} (\mathbf{X}^{(t)} - \mathbf{X}^{(t+K)}) (\mathbf{W} - \mathbf{I}) \mathbf{J} = \mathbf{C}^{(t)} \mathbf{J}.$$

Using the initialization assumption in (3), we have $\mathbf{C}^{(t)} \mathbf{J} = \mathbf{C}^{(0)} \mathbf{J} = \mathbf{0}$. Similarly, we have $\mathbf{D}^{(t)} \mathbf{J} = \mathbf{D}^{(0)} \mathbf{J} = \mathbf{0}$.

Lemma A.4: Using Assumption 2 and Young's Inequality we have

$$\begin{aligned} \mathbb{E} \left\| \nabla_x f(\bar{\mathbf{x}}^{(t)}, \bar{\mathbf{y}}^{(t)}) \right\|^2 &\leq 2\ell^2 \delta_t + 2\mathbb{E} \left\| \nabla \Phi(\bar{\mathbf{x}}^{(t)}) \right\|^2, \\ \mathbb{E} \left\| \nabla_y f(\bar{\mathbf{x}}^{(t)}, \bar{\mathbf{y}}^{(t)}) \right\|^2 &\leq \ell^2 \delta_t. \end{aligned}$$

Proof. We can write

$$\begin{aligned} \mathbb{E} \left\| \nabla_x f(\bar{\mathbf{x}}^{(t)}, \bar{\mathbf{y}}^{(t)}) \right\|^2 &= \mathbb{E} \left\| \nabla_x f(\bar{\mathbf{x}}^{(t)}, \bar{\mathbf{y}}^{(t)}) - \nabla_x f(\bar{\mathbf{x}}^{(t)}, \hat{\mathbf{y}}^{(t)}) + \nabla_x f(\bar{\mathbf{x}}^{(t)}, \hat{\mathbf{y}}^{(t)}) \right\|^2 \\ &\leq 2\ell^2 \mathbb{E} \left\| \bar{\mathbf{y}}^{(t)} - \hat{\mathbf{y}}^{(t)} \right\|^2 + 2\mathbb{E} \left\| \nabla \Phi(\bar{\mathbf{x}}^{(t)}) \right\|^2 = 2\ell^2 \delta_t + 2\mathbb{E} \left\| \nabla \Phi(\bar{\mathbf{x}}^{(t)}) \right\|^2. \end{aligned}$$

Moreover,

$$\mathbb{E} \left\| \nabla_y f(\bar{\mathbf{x}}^{(t)}, \bar{\mathbf{y}}^{(t)}) \right\|^2 = \mathbb{E} \left\| \nabla_y f(\bar{\mathbf{x}}^{(t)}, \bar{\mathbf{y}}^{(t)}) - \nabla_y f(\bar{\mathbf{x}}^{(t)}, \hat{\mathbf{y}}^{(t)}) \right\|^2 \leq \ell^2 \delta_t. \quad (4)$$

The equality in (4) holds due to the fact that $\nabla_y f(\bar{\mathbf{x}}^{(t)}, \hat{\mathbf{y}}^{(t)}) = 0$.

Lemma A.5: Under the assumption that $\eta_c, \eta_d \leq \frac{1}{8KL}$, we can bound the local drift for variables \mathbf{x} and \mathbf{y} as follows

$$\begin{aligned} \mathcal{E}_t^x &\leq 3K\Xi_t^x + 12K^2\eta_c^2\ell^2\mathcal{E}_t^y + 12K^3\eta_c^2\ell^2\gamma_t^x + 12K^3\eta_c^2\ell^2\delta_t + 12K^3\eta_c^2\mathbb{E} \left\| \nabla \Phi(\bar{\mathbf{x}}^{(t)}) \right\|^2 + 3K^2\eta_c^2\sigma^2, \\ \mathcal{E}_t^y &\leq 3K\Xi_t^y + 12K^2\eta_d^2\ell^2\mathcal{E}_t^x + 12K^3\eta_d^2\ell^2\gamma_t^y + 6K^3\eta_d^2\ell^2\delta_t + 3K^2\eta_d^2\sigma^2. \end{aligned}$$

Proof. For $K = 1$ the inequalities obviously hold since $\mathcal{E}_t^x = \Xi_t^x = \frac{1}{n} \mathbb{E} \left\| \mathbf{X}^{(t)} - \bar{\mathbf{X}}^{(t)} \right\|_F^2$ and $\mathcal{E}_t^y = \Xi_t^y =$

$\frac{1}{n}\mathbb{E}\|\mathbf{Y}^{(t)} - \bar{\mathbf{Y}}^{(t)}\|_F^2$ and other terms on the RHSs are positive. For $K \geq 2$ we have

$$\begin{aligned}
ne_{k,t}^x &:= \mathbb{E}\|\mathbf{X}^{(t+k)} - \bar{\mathbf{X}}^{(t)}\|_F^2 \\
&= \mathbb{E}\|\mathbf{X}^{(t+k-1)} - \eta_c \left(\nabla_x F \left(\mathbf{X}^{(t+k-1)}, \mathbf{Y}^{(t+k-1)}; \xi^{(t+k-1)} \right) + \mathbf{C}^{(t)} \right) - \bar{\mathbf{X}}^{(t)}\|_F^2 \\
&\leq \left(1 + \frac{1}{K-1} \right) \mathbb{E}\|\mathbf{X}^{(t+k-1)} - \bar{\mathbf{X}}^{(t)}\|_F^2 + n\eta_c^2\sigma^2 + K\eta_c^2\mathbb{E}\|\nabla_x f \left(\mathbf{X}^{(t+k-1)}, \mathbf{Y}^{(t+k-1)} \right) \\
&\quad - \nabla_x f \left(\bar{\mathbf{X}}^{(t)}, \bar{\mathbf{Y}}^{(t)} \right) + \mathbf{C}^{(t)} + \nabla_x f \left(\bar{\mathbf{X}}^{(t)}, \bar{\mathbf{Y}}^{(t)} \right) (\mathbf{I} - \mathbf{J}) + \nabla_x f \left(\bar{\mathbf{X}}^{(t)}, \bar{\mathbf{Y}}^{(t)} \right) \mathbf{J}\|_F^2 \\
&\leq \underbrace{\left(1 + \frac{1}{K-1} + 4K\eta_c^2\ell^2 \right)}_{:=\mathcal{C}} \mathbb{E}\|\mathbf{X}^{(t+k-1)} - \bar{\mathbf{X}}^{(t)}\|_F^2 + 4K\eta_c^2\ell^2\mathbb{E}\|\mathbf{Y}^{(t+k-1)} - \bar{\mathbf{Y}}^{(t)}\|_F^2 \\
&\quad + 4K\eta_c^2\ell^2n\gamma_t^x + 2K\eta_c^2n\mathbb{E}\|\nabla_x f \left(\bar{\mathbf{x}}^{(t)}, \bar{\mathbf{y}}^{(t)} \right)\|_F^2 + n\eta_c^2\sigma^2 \\
&\leq \mathcal{C}^k\mathbb{E}\|\mathbf{X}^{(t)} - \bar{\mathbf{X}}^{(t)}\|_F^2 + \sum_{r=0}^{k-1} \mathcal{C}^r \left(4K\eta_c^2\ell^2\mathbb{E}\|\mathbf{Y}^{(t+k-1)} - \bar{\mathbf{Y}}^{(t)}\|_F^2 + 4K\eta_c^2\ell^2n\gamma_t^x \right. \\
&\quad \left. + 2K\eta_c^2n\mathbb{E}\|\nabla_x f \left(\bar{\mathbf{x}}^{(t)}, \bar{\mathbf{y}}^{(t)} \right)\|_F^2 + n\eta_c^2\sigma^2 \right)
\end{aligned}$$

If the condition $\eta_c \leq \frac{1}{8KL}$ holds, then it follows that $4K(\eta_c L)^2 \leq \frac{1}{16K} < \frac{1}{16(K-1)}$. Given $\mathcal{C} > 1$, it can be established that $\mathcal{C}^k \leq \mathcal{C}^K \leq \left(1 + \frac{1}{K-1} + \frac{1}{16(K-1)} \right)^K \leq e^{1+\frac{1}{16}} \leq 3$, and $\sum_{r=0}^{k-1} \mathcal{C}^r \leq K\mathcal{C}^K \leq 3K$. Now, we can obtain a bound on client drift for variable \mathbf{x}

$$\mathcal{E}_t^x = \sum_{k=0}^{K-1} e_{k,t}^x \leq 3K\Xi_t^x + 12K^2\eta_c^2\ell^2\mathcal{E}_t^y + 12K^3\eta_c^2\ell^2\gamma_t^x + 6K^3\eta_c^2\mathbb{E}\|\nabla_x f \left(\bar{\mathbf{x}}^{(t)}, \bar{\mathbf{y}}^{(t)} \right)\|_F^2 + 3K^2\eta_c^2\sigma^2. \quad (5)$$

Similarly, a bound on client drift for variable \mathbf{y} can be formulated by

$$\mathcal{E}_t^y = \sum_{k=0}^{K-1} e_{k,t}^y \leq 3K\Xi_t^y + 12K^2\eta_d^2\ell^2\mathcal{E}_t^x + 12K^3\eta_d^2\ell^2\gamma_t^y + 6K^3\eta_d^2\mathbb{E}\|\nabla_y f \left(\bar{\mathbf{x}}^{(t)}, \bar{\mathbf{y}}^{(t)} \right)\|_F^2 + 3K^2\eta_d^2\sigma^2. \quad (6)$$

Using Lemma A.4 in (5) and (6) will complete the proof.

Lemma A.6: We have the following bounds on client variance for variable \mathbf{x} and \mathbf{y}

$$\begin{aligned}
\Xi_{t+1}^x &\leq \left(1 - \frac{p}{2} \right) \Xi_t^x + \frac{6K\eta_x^2\ell^2}{p} (\mathcal{E}_t^x + \mathcal{E}_t^y) + \frac{6K^2\eta_x^2\ell^2}{p} \gamma_t^x + K\eta_x^2\sigma^2, \\
\Xi_{t+1}^y &\leq \left(1 - \frac{p}{2} \right) \Xi_t^y + \frac{6K\eta_y^2\ell^2}{p} (\mathcal{E}_t^x + \mathcal{E}_t^y) + \frac{6K^2\eta_y^2\ell^2}{p} \gamma_t^y + K\eta_y^2\sigma^2.
\end{aligned}$$

Proof. Using the update rule $\mathbf{X}^{(t+1)} = \mathbf{X}^{(t)} - \eta_x \sum_{k=0}^{K-1} \left(\nabla_x F \left(\mathbf{X}^{(t+k)}, \mathbf{Y}^{(t+k)}; \xi^{(t+k)} \right) + \mathbf{C}^{(t)} \right)$ derived

from Algorithm 1, we can bound the client variance for variable \mathbf{x}

$$\begin{aligned}
n\Xi_{t+1}^x &= \mathbb{E} \left\| \mathbf{X}^{(t+1)} - \bar{\mathbf{X}}^{(t+1)} \right\|^2 \\
&= \mathbb{E} \left\| \left(\mathbf{X}^{(t)} - \eta_x \sum_{k=0}^{K-1} \left(\nabla_x F \left(\mathbf{X}^{(t)+k}, \mathbf{Y}^{(t)+k}; \xi^{(t)+k} \right) + \mathbf{C}^{(t)} \right) \right) (\mathbf{W} - \mathbf{J}) \right\|_F^2 \\
&\stackrel{(a)}{\leq} (1-p) \mathbb{E} \left\| \left(\mathbf{X}^{(t)} - \eta_x \sum_{k=0}^{K-1} \left(\nabla_x f \left(\mathbf{X}^{(t)+k}, \mathbf{Y}^{(t)+k} \right) + \mathbf{C}^{(t)} \right) \right) (\mathbf{I} - \mathbf{J}) \right\|_F^2 + nK\eta_x^2\sigma^2 \\
&\leq nK\eta_x^2\sigma^2 + (1+\alpha)(1-p) \mathbb{E} \left\| \mathbf{X}^{(t)} (\mathbf{I} - \mathbf{J}) \right\|_F^2 \\
&\quad + \left(1 + \frac{1}{\alpha} \right) \eta_x^2 \mathbb{E} \left\| \sum_{k=0}^{K-1} \nabla_x f \left(\mathbf{X}^{(t)+k}, \mathbf{Y}^{(t)+k} \right) (\mathbf{I} - \mathbf{J}) - K \nabla_x f \left(\bar{\mathbf{X}}^{(t)}, \bar{\mathbf{Y}}^{(t)} \right) (\mathbf{I} - \mathbf{J}) \right. \\
&\quad \left. + K \nabla_x f \left(\bar{\mathbf{X}}^{(t)}, \bar{\mathbf{Y}}^{(t)} \right) (\mathbf{I} - \mathbf{J}) + K \mathbf{C}^{(t)} \right\|_F^2 \\
&\stackrel{\alpha=\frac{p}{2}, p \leq 1}{\leq} nK\eta_x^2\sigma^2 + \left(1 - \frac{p}{2} \right) \mathbb{E} \left\| \mathbf{X}^{(t)} - \bar{\mathbf{X}}^{(t)} \right\|_F^2 \\
&\quad + \frac{6}{p} \left(K\eta_x^2\ell^2 \|\mathbf{I} - \mathbf{J}\|^2 \left(\sum_{k=0}^{K-1} \left\| \mathbf{X}^{(t)+k} - \bar{\mathbf{X}}^{(t)} \right\|_F^2 + \sum_{k=0}^{K-1} \mathbb{E} \left\| \mathbf{Y}^{(t)+k} - \bar{\mathbf{Y}}^{(t)} \right\|_F^2 \right) \right. \\
&\quad \left. + K^2\eta_x^2 \mathbb{E} \left\| \nabla_x f \left(\bar{\mathbf{X}}^{(t)}, \bar{\mathbf{Y}}^{(t)} \right) (\mathbf{I} - \mathbf{J}) + \mathbf{C}^{(t)} \right\|_F^2 \right) \\
&\leq \left(1 - \frac{p}{2} \right) n\Xi_t^x + \frac{6K\eta_x^2\ell^2}{p} n (\mathcal{E}_t^x + \mathcal{E}_t^y) + \frac{6K^2\eta_x^2\ell^2}{p} n\gamma_t^x + nK\eta_x^2\sigma^2.
\end{aligned}$$

where we used Assumption 1 in (a). Similarly, we can derive an upper bound on client variance for variable \mathbf{y} , thereby concluding the proof.

Lemma A.7: The sum of averaged progress between communications for variables \mathbf{x} and \mathbf{y} can be bounded by

$$\begin{aligned}
\Delta_{t+1}^x + \Delta_{t+1}^y &\leq 2K\ell^2 (\eta_x^2 + \eta_y^2) (\mathcal{E}_t^x + \mathcal{E}_t^y) + 2K^2\ell^2 (2\eta_x^2 + \eta_y^2) \delta_t + 4K^2\eta_x^2 \mathbb{E} \left\| \nabla \Phi \left(\bar{\mathbf{x}}^{(t)} \right) \right\|^2 \\
&\quad + \frac{K\sigma^2}{n} (\eta_x^2 + \eta_y^2).
\end{aligned}$$

Proof. First, we derive an upper bound on the averaged progress for variable \mathbf{x} as follows

$$\begin{aligned}
\Delta_{t+1}^x &:= \mathbb{E} \left\| \bar{\mathbf{x}}^{(t+1)} - \bar{\mathbf{x}}^{(t)} \right\|^2 \\
&= \eta_x^2 \mathbb{E} \left\| \frac{1}{n} \sum_{i,k} \nabla_x F_i \left(\mathbf{x}_i^{(t)+k}, \mathbf{y}_i^{(t)+k}; \xi^{(t)+k} \right) + \frac{K}{n} \sum_i \mathbf{c}_i^{(t)} \right\|^2 \\
&\stackrel{(a)}{\leq} \frac{2K\eta_x^2}{n} \sum_{i,k} \mathbb{E} \left\| \nabla_x f_i \left(\mathbf{x}_i^{(t)+k}, \mathbf{y}_i^{(t)+k} \right) - \nabla_x f_i \left(\bar{\mathbf{x}}_i^{(t)}, \bar{\mathbf{y}}_i^{(t)} \right) \right\|^2 + 2K^2\eta_x^2 \mathbb{E} \left\| \nabla_x f \left(\bar{\mathbf{x}}_i^{(t)}, \bar{\mathbf{y}}_i^{(t)} \right) \right\|^2 \\
&\quad + \frac{K\eta_x^2\sigma^2}{n} \\
&\leq \frac{2K\eta_x^2\ell^2}{n} \sum_{i,k} \left(\mathbb{E} \left\| \mathbf{x}_i^{(t)+k} - \bar{\mathbf{x}}^{(t)} \right\|^2 + \mathbb{E} \left\| \mathbf{y}_i^{(t)+k} - \bar{\mathbf{y}}^{(t)} \right\|^2 \right) + 2K^2\eta_x^2 \mathbb{E} \left\| \nabla_x f \left(\bar{\mathbf{x}}_i^{(t)}, \bar{\mathbf{y}}_i^{(t)} \right) \right\|^2 \\
&\quad + \frac{K\eta_x^2\sigma^2}{n} \\
&\stackrel{(b)}{\leq} 2K\eta_x^2\ell^2 (\mathcal{E}_t^x + \mathcal{E}_t^y) + 2K^2\eta_x^2 \left(2\ell^2 \delta_t + 2\mathbb{E} \left\| \nabla \Phi \left(\bar{\mathbf{x}}^{(t)} \right) \right\|^2 \right) + \frac{K\eta_x^2\sigma^2}{n}. \tag{7}
\end{aligned}$$

Similar to the above derivations, we have

$$\begin{aligned}\Delta_{t+1}^y &:= \mathbb{E} \left\| \bar{\mathbf{y}}^{(t+1)} - \bar{\mathbf{y}}^{(t)} \right\|^2 \leq 2K^2 \eta_y^2 \ell^2 (\mathcal{E}_t^x + \mathcal{E}_t^y) + 2K^2 \eta_y^2 \mathbb{E} \left\| \nabla_y f \left(\bar{\mathbf{x}}_i^{(t)}, \bar{\mathbf{y}}_i^{(t)} \right) \right\|^2 + \frac{K \eta_y^2 \sigma^2}{n} \\ &\stackrel{(c)}{\leq} 2K \eta_y^2 \ell^2 (\mathcal{E}_t^x + \mathcal{E}_t^y) + 2K^2 \eta_y^2 \ell^2 \delta_t + \frac{K \eta_y^2 \sigma^2}{n}.\end{aligned}\quad (8)$$

We used Lemma A.3, A.4, and A.4 in (a), (b), and (c), respectively. Combining (7) and (8) completes the proof.

Lemma A.8: Assuming that $\eta_x, \eta_y \leq \frac{\sqrt{p}}{\sqrt{24K\ell}}$, we have the following bounds on the quality of correction for variables \mathbf{x} and \mathbf{y}

$$\gamma_{t+1}^x \leq \left(1 - \frac{p}{2}\right) \gamma_t^x + \frac{25}{pK} (\mathcal{E}_t^x + \mathcal{E}_t^y) + \frac{12K^2 \ell^2}{p} (2\eta_x^2 + \eta_y^2) \delta_t + \frac{24K^2 \eta_x^2}{p} \mathbb{E} \left\| \nabla \Phi \left(\bar{\mathbf{x}}^{(t)} \right) \right\|^2 + \frac{2\sigma^2}{K\ell^2}, \quad (9)$$

$$\gamma_{t+1}^y \leq \left(1 - \frac{p}{2}\right) \gamma_t^y + \frac{25}{pK} (\mathcal{E}_t^x + \mathcal{E}_t^y) + \frac{12K^2 \ell^2}{p} (2\eta_x^2 + \eta_y^2) \delta_t + \frac{24K^2 \eta_x^2}{p} \mathbb{E} \left\| \nabla \Phi \left(\bar{\mathbf{x}}^{(t)} \right) \right\|^2 + \frac{2\sigma^2}{K\ell^2}. \quad (10)$$

Proof. We can write that

$$\begin{aligned}n\ell^2 \gamma_{t+1}^x &:= \mathbb{E} \left\| \mathbf{C}^{(t+1)} + \nabla_x f \left(\bar{\mathbf{X}}^{(t+1)}, \bar{\mathbf{Y}}^{(t+1)} \right) (\mathbf{I} - \mathbf{J}) \right\|_F^2 \\ &= \mathbb{E} \left\| \mathbf{C}^{(t)} \mathbf{W} + \frac{1}{K} \sum_{k=0}^{K-1} \nabla_x f \left(\mathbf{X}^{(t)+k}, \mathbf{Y}^{(t)+k}, \xi^{(t)+k} \right) (\mathbf{W} - \mathbf{I}) + \nabla_x f \left(\bar{\mathbf{X}}^{(t+1)}, \bar{\mathbf{Y}}^{(t+1)} \right) (\mathbf{I} - \mathbf{J}) \right\|_F^2 \\ &\leq \mathbb{E} \left\| \left(\mathbf{C}^{(t)} + \nabla_x f \left(\bar{\mathbf{X}}^{(t)}, \bar{\mathbf{Y}}^{(t)} \right) (\mathbf{I} - \mathbf{J}) \right) \mathbf{W} \right. \\ &\quad \left. + \left(\frac{1}{K} \sum_{k=0}^{K-1} \nabla_x f \left(\mathbf{X}^{(t)+k}, \mathbf{Y}^{(t)+k} \right) - \nabla_x f \left(\bar{\mathbf{X}}^{(t)}, \bar{\mathbf{Y}}^{(t)} \right) \right) (\mathbf{W} - \mathbf{I}) \right. \\ &\quad \left. + \left(\nabla_x f \left(\bar{\mathbf{X}}^{(t+1)}, \bar{\mathbf{Y}}^{(t+1)} \right) - \nabla_x f \left(\bar{\mathbf{X}}^{(t)}, \bar{\mathbf{Y}}^{(t)} \right) \right) (\mathbf{I} - \mathbf{J}) \right\|_F^2 + \frac{n\sigma^2}{K} \\ &\stackrel{(a)}{\leq} (1 + \alpha)(1 - p)n\ell^2 \gamma_t^x \\ &\quad + 2 \left(1 + \frac{1}{\alpha}\right) \left(\|\mathbf{W} - \mathbf{I}\|^2 \frac{\ell^2}{K} \sum_{k=0}^{K-1} \left(\mathbb{E} \left\| \mathbf{X}^{(t)+k} - \bar{\mathbf{X}}^{(t)} \right\|^2 + \mathbb{E} \left\| \mathbf{Y}^{(t)+k} - \bar{\mathbf{Y}}^{(t)} \right\|^2 \right) \right. \\ &\quad \left. + \|\mathbf{I} - \mathbf{J}\|^2 n\ell^2 \left(\mathbb{E} \left\| \bar{\mathbf{x}}^{(t+1)} - \bar{\mathbf{x}}^{(t)} \right\|^2 + \mathbb{E} \left\| \bar{\mathbf{y}}^{(t+1)} - \bar{\mathbf{y}}^{(t)} \right\|^2 \right) \right) + \frac{n\sigma^2}{K} \\ &\stackrel{\alpha = \frac{p}{2}, \frac{1}{p} \geq 1}{\leq} \left(1 - \frac{p}{2}\right) n\ell^2 \gamma_t^x + \frac{6}{p} \left(\frac{4\ell^2 n}{K} (\mathcal{E}_t^x + \mathcal{E}_t^y) + n\ell^2 (\Delta_{t+1}^x + \Delta_{t+1}^y) \right) + \frac{n\sigma^2}{K}.\end{aligned}$$

In (a) we applied Assumption 1 and the fact that

$$\left(\mathbf{C}^{(t)} + \nabla_x f \left(\bar{\mathbf{X}}^{(t)}, \bar{\mathbf{Y}}^{(t)} \right) (\mathbf{I} - \mathbf{J}) \right) \mathbf{J} = \mathbf{C}^{(t)} \mathbf{J} + \nabla_x f \left(\bar{\mathbf{X}}^{(t)}, \bar{\mathbf{Y}}^{(t)} \right) (\mathbf{J} - \mathbf{J}) \stackrel{\text{Lemma A.3}}{=} \mathbf{0}.$$

Using Lemma A.7 to bound $\Delta_{t+1}^x + \Delta_{t+1}^y$ we have

$$\begin{aligned}\gamma_{t+1}^x &\leq \left(1 - \frac{p}{2}\right) \gamma_t^x + \frac{1}{p} \left(\frac{24}{K} + 12K\eta_x^2 \ell^2 + 12K\eta_y^2 \ell^2 \right) (\mathcal{E}_t^x + \mathcal{E}_t^y) + \frac{12K^2 \ell^2}{p} (2\eta_x^2 + \eta_y^2) \delta_t \\ &\quad + \frac{24K^2 \eta_x^2}{p} \mathbb{E} \left\| \nabla \Phi \left(\bar{\mathbf{x}}^{(t)} \right) \right\|^2 + \frac{6K\sigma^2 (\eta_x^2 + \eta_y^2)}{np} + \frac{\sigma^2}{K\ell^2}.\end{aligned}$$

Applying the conditions on the step sizes will result in (9). In a similar fashion, we can show (10).

Lemma A.9: Using Proposition 2 and assuming that $\eta_y \leq \frac{1}{K\ell}$, we have the following bound on $\mathbb{E} \left\| \hat{\mathbf{y}}^{(t)} - \bar{\mathbf{y}}^{(t+1)} \right\|^2$ for any $\alpha > 0$:

$$\mathbb{E} \left\| \hat{\mathbf{y}}^{(t)} - \bar{\mathbf{y}}^{(t+1)} \right\|^2 \leq (1 + \alpha)(1 - K\eta_y \mu) \delta_t + \left(1 + \frac{1}{\alpha}\right) \eta_y^2 \ell^2 K (\mathcal{E}_t^x + \mathcal{E}_t^y) + \frac{K \eta_y^2 \sigma^2}{n}.$$

Proof. If we replace $\mathbf{x} = \bar{\mathbf{x}}^{(t)}$, $\mathbf{y} = \bar{\mathbf{y}}^{(t)}$, and $\mathbf{y}' = \hat{\mathbf{y}}^{(t)}$ in Proposition 2, we have

$$\nabla_y f(\bar{\mathbf{x}}^{(t)}, \bar{\mathbf{y}}^{(t)})^\top (\bar{\mathbf{y}}^{(t)} - \hat{\mathbf{y}}^{(t)}) + \frac{1}{2\ell} \left\| \nabla_y f(\bar{\mathbf{x}}^{(t)}, \bar{\mathbf{y}}^{(t)}) \right\|^2 + \frac{\mu}{2} \|\bar{\mathbf{y}}^{(t)} - \hat{\mathbf{y}}^{(t)}\|^2 \leq 0. \quad (11)$$

We can also write that

$$\begin{aligned} & \mathbb{E} \left\| \hat{\mathbf{y}}^{(t)} - \bar{\mathbf{y}}^{(t)} - K\eta_y \nabla_y f(\bar{\mathbf{x}}^{(t)}, \bar{\mathbf{y}}^{(t)}) \right\|^2 \\ &= \mathbb{E} \left\| \hat{\mathbf{y}}^{(t)} - \bar{\mathbf{y}}^{(t)} \right\|^2 - 2K\eta_y \mathbb{E} \left\langle \hat{\mathbf{y}}^{(t)} - \bar{\mathbf{y}}^{(t)}, \nabla_y f(\bar{\mathbf{x}}^{(t)}, \bar{\mathbf{y}}^{(t)}) \right\rangle + K^2 \eta_y^2 \mathbb{E} \left\| \nabla_y f(\bar{\mathbf{x}}^{(t)}, \bar{\mathbf{y}}^{(t)}) \right\|^2 \\ &= \mathbb{E} \left\| \hat{\mathbf{y}}^{(t)} - \bar{\mathbf{y}}^{(t)} \right\|^2 + 2K\eta_y \left(\mathbb{E} \left\langle \bar{\mathbf{y}}^{(t)} - \hat{\mathbf{y}}^{(t)}, \nabla_y f(\bar{\mathbf{x}}^{(t)}, \bar{\mathbf{y}}^{(t)}) \right\rangle + \frac{K\eta_y}{2} \mathbb{E} \left\| \nabla_y f(\bar{\mathbf{x}}^{(t)}, \bar{\mathbf{y}}^{(t)}) \right\|^2 \right) \\ &\stackrel{(a)}{\leq} \mathbb{E} \left\| \hat{\mathbf{y}}^{(t)} - \bar{\mathbf{y}}^{(t)} \right\|^2 + 2K\eta_y \left(-\frac{\mu}{2} \mathbb{E} \left\| \hat{\mathbf{y}}^{(t)} - \bar{\mathbf{y}}^{(t)} \right\|^2 \right) = (1 - K\eta_y \mu) \delta_t. \end{aligned}$$

In (a), we used the assumption that $\eta_y \leq \frac{1}{K\ell}$ and (11). Now, we can write

$$\begin{aligned} & \mathbb{E} \left\| \hat{\mathbf{y}}^{(t)} - \bar{\mathbf{y}}^{(t+1)} \right\|^2 \stackrel{(b)}{=} \mathbb{E} \left\| \hat{\mathbf{y}}^{(t)} - \bar{\mathbf{y}}^{(t)} - \frac{\eta_y}{n} \sum_{i,k} \nabla_y F_i(\mathbf{x}_i^{(t)+k}, \mathbf{y}_i^{(t)+k}; \xi^{(t)+k}) \right\|^2 \\ &\leq \mathbb{E} \left\| \hat{\mathbf{y}}^{(t)} - \bar{\mathbf{y}}^{(t)} - K\eta_y \nabla_y f(\bar{\mathbf{x}}^{(t)}, \bar{\mathbf{y}}^{(t)}) - \frac{\eta_y}{n} \sum_{i,k} \nabla_y f_i(\mathbf{x}_i^{(t)+k}, \mathbf{y}_i^{(t)+k}) \right. \\ &\quad \left. + \frac{\eta_y}{n} \sum_{i,k} \nabla_y f_i(\bar{\mathbf{x}}^{(t)}, \bar{\mathbf{y}}^{(t)}) \right\|^2 + \frac{K\eta_y^2 \sigma^2}{n} \\ &\leq (1 + \alpha) \mathbb{E} \left\| \hat{\mathbf{y}}^{(t)} - \bar{\mathbf{y}}^{(t)} - K\eta_y \nabla_y f(\bar{\mathbf{x}}^{(t)}, \bar{\mathbf{y}}^{(t)}) \right\|^2 + \frac{K\eta_y^2 \sigma^2}{n} \\ &\quad + \left(1 + \frac{1}{\alpha}\right) \frac{\eta_y^2 K}{n} \sum_{i,k} \mathbb{E} \left\| \nabla_y f_i(\mathbf{x}_i^{(t)+k}, \mathbf{y}_i^{(t)+k}) - \nabla_y f_i(\bar{\mathbf{x}}^{(t)}, \bar{\mathbf{y}}^{(t)}) \right\|^2 \\ &\leq (1 + \alpha) (1 - K\eta_y \mu) \delta_t + \left(1 + \frac{1}{\alpha}\right) \eta_y^2 \ell^2 K (\mathcal{E}^x + \mathcal{E}^y) + \frac{K\eta_y^2 \sigma^2}{n}. \end{aligned}$$

where in (b), we used Lemma A.3; i.e., $\frac{1}{n} \sum_i \mathbf{d}_i^{(t)} = \mathbf{0}$.

Lemma A.10: Assuming that $\eta_x \leq \frac{\eta_y}{4\sqrt{6}\kappa^2}$ and $\eta_y \leq \frac{1}{K\ell}$, we have the following bound on δ_t

$$\delta_{t+1} \leq \left(1 - \frac{K\eta_y \ell}{6\kappa}\right) \delta_t + 12\eta_y \ell \kappa (\mathcal{E}_t^x + \mathcal{E}_t^y) + \frac{16\kappa^3 K \eta_x^2}{\eta_y \ell} \mathbb{E} \left\| \nabla \Phi(\bar{\mathbf{x}}^{(t)}) \right\|^2 + \frac{8\eta_y \sigma^2 \kappa}{n\ell}.$$

Proof. We begin the proof by writing that

$$\begin{aligned} \delta_{t+1} &\stackrel{(a)}{\leq} (1 + \beta) \mathbb{E} \left\| \hat{\mathbf{y}}^{(t)} - \bar{\mathbf{y}}^{(t+1)} \right\|^2 + \left(1 + \frac{1}{\beta}\right) \mathbb{E} \left\| \hat{\mathbf{y}}^{(t+1)} - \hat{\mathbf{y}}^{(t)} \right\|^2 \\ &\leq (1 + \beta)(1 + \alpha) (1 - K\eta_y \mu) \delta_t + (1 + \beta) \left(1 + \frac{1}{\alpha}\right) \eta_y^2 \ell^2 K (\mathcal{E}_t^x + \mathcal{E}_t^y) \\ &\quad + \left(1 + \frac{1}{\beta}\right) \kappa^2 \mathbb{E} \left\| \bar{\mathbf{x}}^{(t+1)} - \bar{\mathbf{x}}^{(t)} \right\|^2 + (1 + \beta) \frac{K\eta_y^2 \sigma^2}{n} \\ &\stackrel{(b)}{\leq} \left(1 - \frac{K\eta_y \mu}{3}\right) \delta_t + \frac{6\eta_y \ell^2}{\mu} (\mathcal{E}_t^x + \mathcal{E}_t^y) + \frac{4\eta_y \sigma^2}{n\mu} \\ &\quad + \frac{4\kappa^2}{K\eta_y \mu} \left(2K\eta_x^2 \ell^2 (\mathcal{E}_t^x + \mathcal{E}_t^y) + 4K^2 \ell^2 \eta_x^2 \delta_t + 4K^2 \eta_x^2 \mathbb{E} \left\| \nabla \Phi(\bar{\mathbf{x}}^{(t)}) \right\|^2 + \frac{K\eta_x^2 \sigma^2}{n}\right) \\ &= \left(1 - \frac{K\eta_y \ell}{3\kappa} + \frac{16\ell\kappa^3 K \eta_x^2}{\eta_y}\right) \delta_t + \left(\frac{8\ell\kappa^3 \eta_x^2}{\eta_y} + 6\eta_y \ell \kappa\right) (\mathcal{E}_t^x + \mathcal{E}_t^y) + \frac{16\kappa^3 K \eta_x^2}{\eta_y \ell} \mathbb{E} \left\| \nabla \Phi(\bar{\mathbf{x}}^{(t)}) \right\|^2 \\ &\quad + \frac{4\kappa^3 \eta_x^2 \sigma^2}{n\eta_y \ell} + \frac{4\eta_y \sigma^2 \kappa}{n\ell}. \end{aligned}$$

Using the assumption $\eta_x \leq \frac{\eta_y}{4\sqrt{6}\kappa^2}$ completes the proof. In (a), we used the bound in Lemma A.9 for

the first term and Proposition 1 for the second term. In (b), we replaced $\alpha = \beta = \frac{K\eta_y\mu}{3}$ and used (7) in Lemma A.7.

Lemma A.11: Assuming that $\eta_x \leq \frac{1}{16K\ell\kappa}$, we have the following bound on $\mathbb{E}\Phi(\bar{\mathbf{x}}^{(t+1)})$ as follows

$$\mathbb{E}\Phi(\bar{\mathbf{x}}^{(t+1)}) \leq \mathbb{E}\Phi(\bar{\mathbf{x}}^{(t)}) + 2\eta_x\ell^2(\mathcal{E}_t^x + \mathcal{E}_t^y) + 2\ell^2\eta_x K\delta_t - \frac{\eta_x K}{4}\mathbb{E}\|\nabla\Phi(\bar{\mathbf{x}}^{(t)})\|^2 + \frac{K\eta_x^2\ell\sigma^2\kappa}{n}.$$

Proof. According to the Proposition 1, $\Phi(\cdot)$ is $2\kappa\ell$ -smooth, which results in the following

$$\begin{aligned} \mathbb{E}\Phi(\bar{\mathbf{x}}^{(t+1)}) &= \mathbb{E}\Phi\left(\bar{\mathbf{x}}^{(t)} - \frac{\eta_x}{n}\sum_{i,k}\left(\nabla_x F_i(\mathbf{x}_i^{(t)+k}, \mathbf{y}_i^{(t)+k}; \xi_i^{(t)+k}) + \mathbf{c}_i^{(t)}\right)\right) \\ &\leq \mathbb{E}\Phi(\bar{\mathbf{x}}^{(t)}) + \underbrace{\mathbb{E}\left\langle \nabla\Phi(\bar{\mathbf{x}}^{(t)}), -\frac{\eta_x}{n}\sum_{i,k}\left(\nabla_x F_i(\mathbf{x}_i^{(t)+k}, \mathbf{y}_i^{(t)+k}; \xi_i^{(t)+k}) + \mathbf{c}_i^{(t)}\right)\right\rangle}_{:=U} \\ &\quad + \kappa\ell\mathbb{E}\|\bar{\mathbf{x}}^{(t+1)} - \bar{\mathbf{x}}^{(t)}\|^2. \end{aligned}$$

Now, we derive an upper bound for U as follows

$$\begin{aligned} U &:= \mathbb{E}\left\langle \nabla\Phi(\bar{\mathbf{x}}^{(t)}), -\frac{\eta_x}{n}\sum_{i,k}\left(\nabla_x F_i(\mathbf{x}_i^{(t)+k}, \mathbf{y}_i^{(t)+k}; \xi_i^{(t)+k}) + \mathbf{c}_i^{(t)}\right)\right\rangle \\ &= \mathbb{E}\left\langle \nabla\Phi(\bar{\mathbf{x}}^{(t)}), -\frac{\eta_x}{n}\sum_{i,k}\mathbb{E}_{\xi_i^{(t)+k}}\nabla_x F_i(\mathbf{x}_i^{(t)+k}, \mathbf{y}_i^{(t)+k}; \xi_i^{(t)+k})\right\rangle \\ &= -\eta_x\mathbb{E}\left\langle \nabla\Phi(\bar{\mathbf{x}}^{(t)}), \frac{1}{n}\sum_{i,k}\left(\nabla_x f_i(\mathbf{x}_i^{(t)+k}, \mathbf{y}_i^{(t)+k}) - \nabla_x f_i(\bar{\mathbf{x}}^{(t)}, \bar{\mathbf{y}}^{(t)})\right)\right. \\ &\quad \left. + \nabla_x f_i(\bar{\mathbf{x}}^{(t)}, \bar{\mathbf{y}}^{(t)}) - \nabla_x f_i(\bar{\mathbf{x}}^{(t)}, \hat{\mathbf{y}}^{(t)}) + \nabla_x f_i(\bar{\mathbf{x}}^{(t)}, \hat{\mathbf{y}}^{(t)})\right\rangle \\ &= -K\eta_x\mathbb{E}\|\nabla\Phi(\bar{\mathbf{x}}^{(t)})\|^2 - \frac{\eta_x}{n}\sum_{i,k}\left\langle \nabla\Phi(\bar{\mathbf{x}}^{(t)}), \nabla_x f_i(\mathbf{x}_i^{(t)+k}, \mathbf{y}_i^{(t)+k}) - \nabla_x f_i(\bar{\mathbf{x}}^{(t)}, \bar{\mathbf{y}}^{(t)})\right. \\ &\quad \left. + \nabla_x f_i(\bar{\mathbf{x}}^{(t)}, \bar{\mathbf{y}}^{(t)}) - \nabla_x f_i(\bar{\mathbf{x}}^{(t)}, \hat{\mathbf{y}}^{(t)})\right\rangle \\ &\leq -\frac{K\eta_x}{2}\mathbb{E}\|\nabla\Phi(\bar{\mathbf{x}}^{(t)})\|^2 + \frac{\eta_x}{n}\sum_{i,k}\left(\mathbb{E}\|\nabla_x f_i(\mathbf{x}_i^{(t)+k}, \mathbf{y}_i^{(t)+k}) - \nabla_x f_i(\bar{\mathbf{x}}^{(t)}, \bar{\mathbf{y}}^{(t)})\|^2\right. \\ &\quad \left. + \mathbb{E}\|\nabla_x f_i(\bar{\mathbf{x}}^{(t)}, \bar{\mathbf{y}}^{(t)}) - \nabla_x f_i(\bar{\mathbf{x}}^{(t)}, \hat{\mathbf{y}}^{(t)})\|^2\right) \\ &\leq -\frac{K\eta_x}{2}\mathbb{E}\|\nabla\Phi(\bar{\mathbf{x}}^{(t)})\|^2 + \eta_x\ell^2(\mathcal{E}_t^x + \mathcal{E}_t^y) + K\eta_x\ell^2\delta_t. \end{aligned}$$

Now, we apply the above upper bound for U and (7) in Lemma A.7 as follows

$$\begin{aligned} \mathbb{E}\Phi(\bar{\mathbf{x}}^{(t+1)}) &\leq \mathbb{E}\Phi(\bar{\mathbf{x}}^{(t)}) + \eta_x\ell^2(\mathcal{E}_t^x + \mathcal{E}_t^y) + \ell^2\eta_x K\delta_t - \frac{\eta_x K}{2}\mathbb{E}\|\nabla\Phi(\bar{\mathbf{x}}^{(t)})\|^2 + \kappa\ell\mathbb{E}\|\bar{\mathbf{x}}^{(t+1)} - \bar{\mathbf{x}}^{(t)}\|^2 \\ &\leq \mathbb{E}\Phi(\bar{\mathbf{x}}^{(t)}) + (\eta_x\ell^2 + 2K\eta_x^2\ell^3\kappa)(\mathcal{E}_t^x + \mathcal{E}_t^y) + \frac{K\eta_x^2\ell\kappa\sigma^2}{n} \\ &\quad + (\ell^2\eta_x K + 4K^2\ell^3\eta_x^2\kappa)\delta_t + \left(4K^2\eta_x^2\ell\kappa - \frac{\eta_x K}{2}\right)\mathbb{E}\|\nabla\Phi(\bar{\mathbf{x}}^{(t)})\|^2. \end{aligned}$$

Applying the assumption $\eta_x \leq \frac{1}{16K\ell\kappa}$ completes the proof.

Lemma A.12: Under the assumption that $\eta_d = \Theta(\frac{p}{\kappa K\ell})$, $\eta_c = \Theta(\frac{\eta_d}{\kappa^2})$, and $\eta_s = \eta_r = \Theta(p)$, we can find constants A_x, A_y, B_x, B_y , and C , such that $D_8 > 0$ and $D_9 \geq 0$, and we have

$$\mathcal{H}_{t+1} - \mathcal{H}_t \leq -D_8 K\eta_x\mathbb{E}\|\nabla\Phi(\bar{\mathbf{x}}^{(t)})\|^2 + D_9 K\ell\eta_d^3\sigma^2 + \frac{K\eta_x^2\ell\kappa}{n}\sigma^2 + \frac{8\eta_y}{n\ell Kp}\sigma^2, \quad (12)$$

where

$$\mathcal{H}_t = \mathbb{E}\Phi(\bar{\mathbf{x}}^{(t)}) - \mathbb{E}\Phi(\mathbf{x}^*) + A_x\eta_d\ell\Xi_t^x + A_y\eta_d\ell\Xi_t^y + B_x K^2\ell^3\eta_d^3\gamma_t^x + B_y K^2\ell^3\eta_d^3\gamma_t^y + C\frac{1}{K\kappa p}\delta_t.$$

Proof. According to the Lemma A.5, we have

$$\begin{aligned}
0 &\leq -D_x \frac{\ell}{K} \eta_d \mathcal{E}_t^x + 3D_x \ell \eta_d \Xi_t^x + 12D_x K \eta_c^2 \eta_d \ell^3 \mathcal{E}_t^y + 12D_x K^2 \eta_c^2 \eta_d \ell^3 \gamma_t^x + 12D_x K^2 \eta_c^2 \eta_d \ell^3 \delta_t \\
&\quad + 12D_x K^2 \eta_c^2 \eta_d \ell \mathbb{E} \left\| \nabla \Phi \left(\bar{\mathbf{x}}^{(t)} \right) \right\|^2 + 3D_x K \eta_c^2 \eta_d \ell \sigma^2, \\
0 &\leq -D_y \frac{\ell}{K} \eta_d \mathcal{E}_t^y + 3D_y \ell \eta_d \Xi_t^y + 12D_y K \eta_d^3 \ell^3 \mathcal{E}_t^x + 12D_y K^2 \eta_d^3 \ell^3 \gamma_t^y + 6D_y K^2 \eta_d^3 \ell^3 \delta_t + 3D_y K \eta_d^3 \ell \sigma^2.
\end{aligned} \tag{13}$$

By applying the definition of \mathcal{H}_t from (12) and using (13), Lemmas A.5, A.6, A.8, A.10, and A.11, we have

$$\begin{aligned}
\mathcal{H}_{t+1} - \mathcal{H}_t &\leq \underbrace{\left(-B_x \frac{p}{2} + A_x \frac{6\eta_s^2}{p} + D_x 12 \right)}_{\leq D_1} \eta_d^3 K^2 \ell^3 \gamma_t^x \\
&\quad + \underbrace{\left(-B_y \frac{p}{2} + A_y \frac{6\eta_r^2}{p} + D_y 12 \right)}_{\leq D_2} \eta_d^3 K^2 \ell^3 \gamma_t^y \\
&\quad + \underbrace{\left(-A_x \frac{p}{2} + 3D_x \right)}_{\leq D_3} \Xi_t^x \eta_d \ell \\
&\quad + \underbrace{\left(-A_y \frac{p}{2} + 3D_y \right)}_{\leq D_4} \Xi_t^y \eta_d \ell \\
&\quad + \underbrace{\left(-D_x + A_x \frac{6K^2 \ell^2 \eta_x^2}{p} + A_y \frac{6K^2 \ell^2 \eta_y^2}{p} + B_x \frac{25\eta_d^2 \ell^2 K^2}{p} + B_y \frac{25\eta_d^2 \ell^2 K^2}{p} + D_y 12K^2 \ell^2 \eta_d^2 + 2\eta_x K \ell + C \frac{12\eta_r}{p} \right)}_{\leq D_5} \frac{\ell}{K} \eta_d \mathcal{E}_t^x \\
&\quad + \underbrace{\left(-D_y + A_x \frac{6K^2 \ell^2 \eta_x^2}{p} + A_y \frac{6K^2 \ell^2 \eta_y^2}{p} + B_x \frac{25\eta_d^2 \ell^2 K^2}{p} + B_y \frac{25\eta_d^2 \ell^2 K^2}{p} + D_x 12K^2 \ell^2 \eta_c^2 + 2\eta_x K \ell + C \frac{12\eta_r}{p} \right)}_{\leq D_6} \frac{\ell}{K} \eta_d \mathcal{E}_t^y \\
&\quad + \underbrace{\left(-C \frac{\eta_r}{6p} + B_x \frac{12K^4 \ell^4}{p} \eta_d^2 (3\eta_y^2) \kappa^2 + B_y \frac{12K^4 \ell^4}{p} \eta_d^2 (3\eta_x^2) \kappa^2 + D_x 12K^2 \ell^2 \eta_c^2 \kappa^2 + D_y 6K^2 \ell^2 \eta_d^2 \kappa^2 + 2\ell K \kappa^2 \frac{\eta_x}{\eta_d} \right)}_{\leq D_7} \frac{\ell \eta_d}{\kappa^2} \delta_t \\
&\quad + \underbrace{\left(-\frac{1}{4} + B_x \frac{24K^3 \ell^3}{p} \eta_d^3 \eta_x + B_y \frac{24K^3 \ell^3}{p} \eta_d^3 \eta_y + C \frac{16\kappa^2 \eta_x}{K \ell \eta_y p} + D_x 12K \ell \eta_d \frac{\eta_c}{\eta_s} \right)}_{\leq D_8} K \eta_x \mathbb{E} \left\| \nabla \Phi \left(\bar{\mathbf{x}}^{(t)} \right) \right\|^2 \\
&\quad + \underbrace{\left(A_x \eta_s^2 + A_y \eta_r^2 + B_x 2 + B_y 2 + D_x 3 + D_y 3 \right)}_{\leq D_9} K \ell \eta_d^3 \sigma^2 + \frac{K \eta_x^2 \ell \kappa}{n} \sigma^2 + C \frac{8\eta_y}{n \ell K p} \sigma^2.
\end{aligned}$$

Assuming that $D_x = D_y = v$, as long as $\eta_d \leq \frac{p}{200v\kappa K \ell}$, $\eta_c \leq \frac{\eta_d}{\kappa^2}$, $\eta_s = \eta_r = pv$, $A_x = A_y = \frac{6v}{p}$, $B_x = B_y = \frac{1}{p}(72v^3 + 24v)$, and $C = \frac{1}{24}$, any $v > 1$ can make $D_1, D_2, D_3, D_4, D_5, D_6, D_7 \leq 0$, $D_8 < 0$, and $D_9 \geq 0$.

Proof of Theorem 1. Using the telescopic sum for \mathcal{H}_t , we have

$$\begin{aligned}
\frac{1}{T+1} \sum_{t=0}^T (\mathcal{H}_{t+1} - \mathcal{H}_t) &= \frac{1}{T+1} (\mathcal{H}_{T+1} - \mathcal{H}_0) \\
&\leq -D_8 K \eta_x \frac{1}{T+1} \sum_{t=0}^T \mathbb{E} \left\| \nabla \Phi \left(\bar{\mathbf{x}}^{(t)} \right) \right\|^2 + D_9 K \ell \eta_d^3 \sigma^2 + \frac{K \eta_x^2 \ell \kappa}{n} \sigma^2 + \frac{8\eta_y}{n \ell K p} \sigma^2,
\end{aligned}$$

which results in

$$\frac{1}{T+1} \sum_{t=0}^T \mathbb{E} \left\| \nabla \Phi \left(\bar{\mathbf{x}}^{(t)} \right) \right\|^2 \leq \frac{\mathcal{H}_0 - \mathcal{H}_{T+1}}{(T+1)D_8} \frac{1}{K \eta_x} + \frac{D_9 \ell \eta_d^3 \sigma^2}{D_8 \eta_x} + \frac{\eta_x \ell \kappa}{n D_8} \sigma^2 + \frac{8\eta_y}{n \ell D_8 K^2 p \eta_x}. \tag{14}$$

Now, we want to ensure $\frac{1}{T+1} \sum_{t=0}^T \mathbb{E} \left\| \nabla \Phi \left(\bar{\mathbf{x}}^{(t)} \right) \right\|^2 \leq \epsilon^2$ for any arbitrary $\epsilon > 0$, which is equivalent to bounding each term on the RHS of (14) to the order of ϵ^2 . Given that $D_8 = \Theta(1)$, $D_9 = O\left(\frac{1}{p}\right)$, $\eta_x = \Theta\left(\frac{1}{p}\right)$, and $\eta_y = \Theta\left(\frac{p^2}{\kappa^3 K \ell}\right)$, we have

$$\begin{aligned}
T &= O\left(\frac{\kappa^3}{p^2 \epsilon^2}\right) \mathcal{H}_0 \ell, \\
K &= O\left(\frac{p^2 \sigma^2}{\kappa^2 n \epsilon^2} + \left(1 + \frac{\kappa}{\sqrt{np}}\right) \frac{\sigma}{\epsilon}\right),
\end{aligned}$$

where $\mathcal{H}_0 = O\left(1 + \frac{\delta_0}{K \kappa p}\right)$ and $\delta_0 = O\left(\frac{q}{\mu^2}\right)$.